Inorganic Chemistry, Vol. 16, No. 5, 1977 **1077**

Contribution from the School of Chemical Sciences,
University of Illinois, Urbana, Illinois 61801

Magnetic Exchange Interactions in Transition Metal Dimers. 10. Structural and Magnetic Characterization of the Oxalate-Bridged Complex $[Cu_2(Et_5dien)_2(C_2O_4)](BPh_4)_2$ and Related Copper(II) Dimers. Effects of Nonbridging Ligands and Counterions on Exchange Interactions

TIMOTHY R. FELTHOUSE, EDWARD J. LASKOWSKI, and DAVID N. HENDRICKSON*[1]

Received November 2, 1976 AIC60784Z

The structure of $[Cu_2(Et_5dien)_2(C_2O_4)](BPh_4)_2$, where Et_5dien is 1,1,4,7,7-pentaethyldiethylenetriamine and $C_2O_4^{2-}$ is the dianion of oxalic acid, has been determined using heavy-atom, least-squares, x-ray methods, in conjunction with data measured on a four-circle diffractometer, to give conventional discrepancy factors of $R_F = 0.069$ and $R_{wF} = 0.056$ for 2679 observed ($F_o \geq 3\sigma$) reflections. The compound crystallizes in the monoclinic space group $P2_1/n$ with two formula weights in a cell having the dimensions $a = 9.776$ (5) Å, $b = 25.004$ (12) Å, $c = 14.551$ (6) Å, and $\beta = 91.83$ (2)°. The observed and calculated densities are 1.25 (2) and 1.26 g cm^{-1}, respectively. The compound $[Cu_2(Et_5dien)_2(C_2O_4)](BPh_4)_2$ is a BPh_4^- salt of an oxalate-bridged, centrosymmetric Cu(II) dimeric cation. The oxalate dianion bridges in a bis-bidentate fashion between two distorted trigonal-bipyramidal (TBP) copper complexes with the oxalate dianion taking both an equatorial (Cu–O = 2.174 (4) Å) and an axial (Cu–O = 1.972 (4) Å) coordination site at each Cu(II) ion. The Cu–Cu distance is 5.410 (1) Å and the Cu–(C_2O_4)–Cu unit is planar. Variable-temperature (4.2–270 K) magnetic susceptibility data for this compound show a relatively large antiferromagnetic exchange interaction with a J value of −37.4 cm^{-1}. Magnetic susceptibility data (4.2–270 K) and EPR spectra (X and Q band) are presented for the series of μ-oxalato compounds $[Cu_2(\text{"dien"})_2(C_2O_4)](X)_2$, where "dien" is variously Et_5dien, Me_5dien, dpt (dipropylenetriamine), and dien (diethylenetriamine) and X^- is either BPh_4^-, PF_6^- or ClO_4^-. The Et_5dien compounds have TBP Cu(II) coordination geometries with the largest antiferromagnetic interactions. Replacing Et_5dien by any of the other three "dien" ligands distorts the Cu(II) coordination geometry toward square pyramidal and decreases the antiferromagnetic interaction. A simplified molecular orbital analysis is presented to explain the changes in exchange interactions. The effects of nonbridging "dien" ligand and counterion are explained via the MO analysis. And finally, magnetic susceptibility and EPR data are reported for some analogous squarate ($C_4O_4^{2-}$)-, succinate ($^-O_2CCH_2CH_2CO_2^-$)-, and cyanate (NCO^-)-bridged Cu(II) dimers.

Introduction

Recent work on magnetic exchange interactions in transition metal cluster complexes has focused on Cu(II) and Ni(II) dimers bridged by hydroxide, alkoxide, and halide ions.[2-5] While a number of electronic and structural factors influence an exchange interaction, certain workers[2,3] have identified the bridging angle as the most important factor in di-μ-hydroxo-bridged Cu(II) complexes. Others[4] contended that the "relative symmetry" of the exchanging electrons is the most critical feature in a series of dimeric copper(II) β-polyketonates. In a study of a series of four di-μ-chloro-bridged Cu(II) dimers of both square-pyramidal (SP) and trigonal-bipyramidal (TBP) local copper ion geometries, it was concluded[2] that no apparent correlation existed between the exchange parameter and the bridging angle. The geometrical constraints of the nonbridging ligands gave rise to different copper to ligand plane distances, as well as Cu–Cl(bridge) bond distances. In spite of all of these variables, it seemed to us that the TBP chloride-bridged complexes with d_{z^2} Cu(II) ion ground states exhibited stronger antiferromagnetic exchange interactions than the SP, $d_{x^2-y^2}$ Cu(II) ion ground-state complexes. It is this dependence of the exchange interaction on the Cu(II) single-ion ground state which we shall examine in this paper.

Previously, we reported[6] that an oxalate-bridged Ni(II) dimer has an antiferromagnetic exchange interaction with $J = -17$ cm^{-1}, whereas, for an analogous Cu(II) dimer, $[Cu_2(tren)_2(C_2O_4)](BPh_4)_2$ where tren is 2,2′,2″-triaminotriethylamine and $C_2O_4^{2-}$ is oxalate, no exchange interaction is detectable to 4.2 K in the magnetic susceptibility data. This we explained by noting that the single unpaired electron associated with each pseudooctahedrally coordinated Cu(II) ion is in a d_{z^2} orbital directed perpendicular to the oxalate bridge plane. The recent theoretical work of Hoffmann et al.[7] agreed with our interpretation. Our later work[8,9] on $[Cu_2(dien)_2(C_2O_4)](ClO_4)_2$ and $[Cu_2(dien)_2(C_2O_4)](BPh_4)_2$, where dien is diethylenetriamine, convinced us that it was possible to construct a series of μ-oxalato-copper(II) dimers wherein, by varying the nonbridging ligand, it would be possible to systematically change the local Cu(II) ion geometry. The bis-bidentate oxalate bridge serves as a relatively constant bridging group in respect to the Cu–Cu distance, O–Cu–O angle, and bridging ion dimensions; this constancy is important in checking the dependence of the exchange parameter on the local Cu(II) ion coordination geometry. A systematic change in the local Cu(II) ion geometry appeared to be obtainable by replacing dien in $[Cu_2(dien)_2(C_2O_4)]^{2+}$ with dpt (dipropylenetriamine), Me_5dien (1,1,4,7,7-pentamethyldiethylenetriamine), and Et_5dien (1,1,4,7,7-pentaethyldiethylenetriamine). Since it is known[10] that Et_4dien (1,1,7,7-tetraethyldiethylenetriamine) enforces a TBP geometry about Cu(II), we anticipated a series wherein the Cu(II) ion geometry changes from SP in the crystallographically characterized[11] $[Cu_2(dien)_2(C_2O_4)](ClO_4)_2$ to TBP in the Et_5dien complex.

In this paper we report the results of a structure determination of $[Cu_2(Et_5dien)_2(C_2O_4)](BPh_4)_2$. Variable-temperature (4.2–270 K) magnetic susceptibility and EPR data are presented for a series of μ-oxalato-copper(II) dimers of the composition $[Cu_2(\text{"dien"})_2(C_2O_4)]X_2$, where "dien" is dien, dpt, Me_5dien, or Et_5dien and X^- is variously BPh_4^-, ClO_4^-, or PF_6^-. In some cases, the oxalate bridge was replaced with the squarate ion ($C_4O_4^{2-}$), the succinate ion ($^-O_2CCH_2CH_2CO_2^-$), or two cyanate ions (NCO^-), in part, to better understand the pathways of exchange interaction that are operative in the oxalate complexes and also to ascertain the effects of changing the bridging moiety while maintaining a relatively constant Cu(II) ion coordination geometry. A preliminary report of the structural and magnetic data for $[Cu_2(Et_2dien)_2(C_2O_4)](BPh_4)_2$ has appeared.[12]

Experimental Section

Compound Preparation. The tridentate ligands diethylenetriamine (Union Carbide), dipropylenetriamine (Aldrich), 1,1,4,7,7-pentamethyldiethylenetriamine (Ames Laboratories, Inc.), and

1,1,4,7,7-pentaethyldiethylenetriamine (Ames Laboratories, Inc.) were used as received. Squaric acid (3,4-dihydroxy-3-cyclobutene-1,2-dione) was purchased from Aldrich. Elemental analyses were performed in the microanalytical laboratory of the School of Chemical Sciences, University of Illinois. The analytical data are given in Table I.[13]

Samples of $[Cu_2(dpt)_2(C_2O_4)](ClO_4)_2$, $[Cu_2(Me_5dien)_2(C_2O_4)](ClO_4)_2$, and $[Cu_2(Et_5dien)_2(C_2O_4)](ClO_4)_2$ were prepared by a method analogous to the method given by Curtis.[14]

Preparation of complexes of the type $[Cu_2("dien")_2(C_2O_4)](PF_6)_2$, where "dien" = dien, dpt, Me_5dien, or Et_5dien, was accomplished by the following general procedure. An aqueous suspension of ~0.01 mol of $CuC_2O_4 \cdot {}^1/_2H_2O$ was reacted with ~0.01 mol of the appropriate "dien" ligand. The resulting solution was filtered to remove any undissolved polymer. The solution was concentrated to ~30–40 mL total volume. Addition of ~0.6 g of NH_4PF_6 dissolved in a minimum of water yielded the desired product.

Samples of $[Cu_2("dien")_2(C_2O_4)](BPh_4)_2$, in contrast to a previously reported procedure,[8] were prepared directly from an aqueous mixture of ~0.01 mol of $Cu(ClO_4)_2 \cdot 6H_2O$, ~0.01 mol of "dien", and ~0.005 mol of $Na_2C_2O_4$. Addition of an aqueous solution of $NaBPh_4$ gave the product. This method produces a light green powder of $[Cu_2(Et_5dien)_2(C_2O_4)](BPh_4)_2$. However, slow evaporization of an acetonitrile solution of this compound yields two forms of crystals: either long, thin rectangular green needles or much shorter blue rhombohedral prisms. The formation of one type over another seems to be quite sensitive to the amount of moisture and heat in the environment. Green needles suitable for x-ray work form under conditions of relatively high atmospheric humidity, while the blue crystals can be grown quite readily in a refrigerator or at room temperature but with low humidity. Elemental analyses and infrared spectra of samples of each crystal form do *not* indicate any molecules of solvation.

A squarate-bridged Cu(II) complex was prepared from polymeric $CuC_4O_4 \cdot 2H_2O$.[15] The polymer was suspended in methanol and a slight excess of Et_5dien was added. After being stirred for ~1 h, the solution was filtered and equimolar amounts of $Cu(NO_3)_2 \cdot 3H_2O$ and Et_5dien in methanol were added to the filtrate. Addition of a methanol solution of $NaBPh_4$ gave a fine dark green solid of $[Cu_2(Et_5dien)_2(C_4O_4)](BPh_4)_2$.

A sample of the succinate-bridged $[Cu_2(Me_5dien)_2(O_2CCH_2CH_2CO_2)](BPh_4)_2$ was prepared according to the above procedure used for the C_2O_4–BPh_4 complexes, substituting $Na_2(O_2CCH_2CH_2CO_2) \cdot 6H_2O$ for $Na_2C_2O_4$. $[Cu_2(Et_5dien)_2(O_2CCH_2CH_2CO_2)](BPh_4)_2$ was prepared using the procedure described above for the squarate complex using $Cu(O_2CCH_2CH_2CO_2) \cdot 2H_2O$ instead of $CuC_4O_4 \cdot 2H_2O$.

Samples of $[Cu_2(dpt)_2(NCO)_2](BPh_4)_2$, $[Cu_2(Me_5dien)_2(NCO)_2](BPh_4)_2$, and $[Cu_2(Et_5dien)_2(NCO)_2](BPh_4)_2$ were prepared in an analogous fashion to the method for the oxalate analogues using at least a twofold excess of NaNCO.

A sample of $[Ni_2(dien)_2(OH_2)_2(C_2O_4)](ClO_4)_2$ was prepared by the method described by Curtis.[14]

Physical Measurements. Variable-temperature (4.2–270 K) magnetic susceptibilities were measured with a Princeton Applied Research Model 150A vibrating-sample magnetometer operating at 12.7 kG and calibrated with $CuSO_4 \cdot 5H_2O$ as described in a previous paper.[6] All data were corrected for diamagnetism[16,17] and TIP (taken as 120×10^{-6} cgsu/Cu(II) dimer). Least-squares fittings of the magnetic susceptibilities to the Bleaney–Bowers equation[18] ($\hat{H} = -2J\hat{S}_1 \cdot \hat{S}_2$) were performed with a new version of the minimization computer program STEPT.[19]

EPR spectra of powdered samples were recorded on a Varian E-9 X-band spectrometer and a Varian E-15 Q-band spectrometer operating at 9.1–9.5 and 35 GHz, respectively. The X-band frequency was determined using a Hewlett-Packard Model 5240A 12.4-GHz digital frequency meter while the Q-band frequency was calibrated with DPPH ($g = 2.0036$). X-Band spectra were recorded at ~300, ~80, and 6 K. The lowest temperature was achieved with an Air Products Heli-tran liquid-helium cooling system and was measured with a calibrated carbon resistor. Q-Band spectra were taken at ~300 and ~110 K.

Crystal Measurements. A green rectangular prism of $[Cu_2(Et_5dien)_2(C_2O_4)](BPh_4)_2$ was cleaved along the needle axis and mounted along this axis in a quartz capillary tube. The dimensions of the crystal used in the intensity data collection were $0.29 \times 0.33 \times 0.28$ mm.

Table II. Experimental Data for the X-Ray Diffraction Study of $[Cu_2(Et_5dien)_2(C_2O_4)](BPh_4)_2$

Crystal Parameters	
$a = 9.776$ (5) Å	Space group $P2_1/n$
$b = 25.004$ (12) Å	$Z = 4$ (2 dimers)
$c = 14.551$ (6) Å	Mol wt 1340.46
$\beta = 91.83$ (2)°	ρ(calcd) = 1.26 g cm^{-3}
$V = 3553$ (2) Å^3	ρ(obsd) = 1.25 (2)g cm^{-3} (flotation in toluene-bromotoluene)

Measurement of Intensity Data

Radiation: Mo Kα, λ 0.7107 Å
Monochromator: graphite crystal
Attenuators: copper; attenuation factor ~3
Takeoff angle: 1°
Crystal orientation: mounted along needle axis
Reflections measd: $+h,+k,\pm l$
Max 2θ: 42°
Scan type: θ-2θ scan technique
Scan length: symmetrical scan, $2\theta = 1.1°$; corrected for $K\alpha_1$-$K\alpha_2$ sepn
Background measurement: stationary-crystal, stationary-counter; 10 s each at beginning and end of 2θ scan
Std reflections: three standards [(400), (0,14,0), (006)] measured after every 98 reflections; no systematic change in intensity during data collection
Reflections collected: 3809 unique reflections, 2679 observed above 3σ cutoff
Temperature: 20 °C

Treatment of Intensity Data

Data reduction: by program VANDYPIK
Definition of σ: $\sigma(F_o^2) = (Lp)^{-1}[T_c + 0.25(t_c/t_b)^2(B_1 + B_2) + (0.03I)]^{1/2}$, where T_c is the total counts, (t_c/t_b) is the ratio of time counting peak intensity to that of counting backgrounds, and B_1 and B_2 are background counts; $\sigma(F_o) = \sigma(F_o^2)/2F_o$
Weighting scheme: $w = 2F_o/\sigma(F_o^2)$
Absorption coeff: 6.863 cm^{-1}
Range of transmission factors: 0.799-0.821

Preliminary precession photographs on a different crystal gave approximate unit cell dimensions and showed systematic absences for $0k0$, $k = 2n + 1$, and $h0l$, $h + l = 2n + 1$. The space group was determined to be $P2_1/n$, which is an alternative setting of the conventional space group $P2_1/c$ [C_{2h}^5; No. 14] and has equivalent positions at $\pm(x, y, z)$ and $\pm({}^1/_2 + x, {}^1/_2 - y, {}^1/_2 + z)$.

A computer-controlled Picker FACS-1 diffractometer was used for data collection. The crystal was accurately centered for data collection. Details of the data collection are given in Table II. The unit cell parameters were determined from a least-squares refinement using 12 strong reflections which had been centered by hand. Lorentz and polarization corrections were applied to the data. In view of the small variation in transmission factors (81.0 ± 1.1%) no absorption correction was applied.

Structure Solution and Refinement. Cu, H, N, O and B atoms were assigned scattering factors as given by Hansen et al.[20a] while C was assigned the scattering factors from Cromer and Mann.[20b] The copper ion was corrected for anomalous dispersion.[20c] Programs used in the structure solution include ALF (Fourier synthesis), ORFLS (least-squares data refinement by Busing and Levy), JAM (distances and angles with esd's), BESTP (least-squares planes by M. E. Pippy), HYGEN (hydrogen atom position generation by F. K. Ross), and ORTEP II (thermal ellipsoid drawings by C. K. Johnson).

Using 2679 observed reflections with $F_o \geq 3\sigma$, a three-dimensional Patterson map of $[Cu_2(Et_5dien)_2(C_2O_4)](BPh_4)_2$ was generated. The position of the Cu atom was located and isotropically refined twice. Subsequently, three successive Fourier maps were used to locate 44 of the 46 nonhydrogen atoms. The remaining two atoms, the carbon atoms of an ethyl group, were found from a difference Fourier map. Refinement proceeded using full-matrix least-squares treatment of the overall scale factor and the individual positional and isotropic thermal parameters for all 46 nonhydrogen atoms in the asymmetric unit. The function minimized was $\sum w||F_o| - |F_c||^2$ where $w = 1/(\sigma(F_o))^2$. Five cycles of refinement led to an isotropic convergence with $R_F = 0.124$ and $R_{wF} = 0.121$ ($R_F = \sum(|F_o| - |F_c|)/\sum|F_o|$ and $R_{wF} = (\sum w|F_o - F_c|^2/\sum wF_o^2)^{1/2}$). Due to the limitation on the number of variable parameters which could be handled by ORFLS, each cycle of anisotropic refinement was carried out in two parts. First, the cation

Table III. Final Positional Parameters for All Atoms in $[Cu_2(Et_5dien)(C_2O_4)](BPh_4)_2$,[a] Including Isotropic Temperature Factors for Hydrogen Atoms[b]

Atom	x/a	y/b	z/c	Atom	x/a	y/b	z/c	B, Å²
Cu	0.155 25 (9)	0.065 47 (3)	0.108 38 (6)	H(5)	0.1462	0.1372	0.3300	6.45
O(1)	0.176 1 (5)	0.003 4 (2)	0.026 3 (3)	H(6)	0.2706	0.1074	0.2907	6.45
O(2)	−0.057 2 (4)	0.053 6 (2)	0.064 3 (3)	H(7)	0.0078	0.0618	0.2971	7.35
C(5)	0.065 8 (7)	−0.014 6 (3)	−0.011 8 (5)	H(8)	0.1269	0.0462	0.3648	7.35
N(1)	0.131 7 (8)	0.130 7 (2)	0.187 3 (4)	H(9)	−0.0151	0.1819	0.2316	5.85
N(2)	0.313 1 (6)	0.107 5 (2)	0.048 0 (4)	H(10)	−0.0735	0.1264	0.2035	5.85
N(3)	0.150 3 (8)	0.018 6 (2)	0.235 9 (4)	H(11)	−0.1523	0.1908	0.0974	5.95
C(1)	0.234 (1)	0.170 8 (3)	0.162 3 (5)	H(12)	−0.0026	0.2055	0.0756	5.95
C(2)	0.341 (1)	0.150 5 (4)	0.112 5 (9)	H(13)	−0.0610	0.1499	0.0475	5.95
C(3)	0.168 (1)	0.112 2 (4)	0.283 3 (6)	H(14)	0.3667	0.1451	−0.0618	10.65
C(4)	0.109 (1)	0.059 3 (4)	0.302 4 (5)	H(15)	0.2310	0.1656	−0.0220	10.65
C(50)	−0.009 (1)	0.153 6 (3)	0.185 7 (6)	H(16)	0.1921	0.1307	−0.1623	8.52
C(51)	−0.060 0 (9)	0.176 2 (3)	0.096 4 (6)	H(17)	0.2530	0.0763	−0.1298	8.52
C(52)	0.281 (1)	0.130 3 (6)	−0.039 9 (9)	H(18)	0.1172	0.0968	−0.0901	8.52
C(53)	0.203 (1)	0.109 8 (4)	−0.107 8 (6)	H(19)	0.4205	0.0450	0.0046	6.97
C(54)	0.436 2 (9)	0.075 2 (3)	0.047 6 (6)	H(20)	0.4519	0.0580	0.1074	6.97
C(55)	0.567 0 (9)	0.101 8 (4)	0.022 1 (7)	H(21)	0.6457	0.0780	0.0214	7.43
C(56)	0.046 3 (9)	−0.023 5 (4)	0.232 1 (5)	H(22)	0.5596	0.1174	−0.0390	7.43
C(57)	0.024 (1)	−0.055 5 (4)	0.318 7 (6)	H(23)	0.5910	0.1305	0.0637	7.43
C(58)	0.286 (1)	−0.002 5 (4)	0.265 0 (6)	H(24)	0.0653	−0.0489	0.1815	5.76
C(59)	0.337 (1)	−0.046 9 (4)	0.207 4 (7)	H(25)	−0.0418	−0.0078	0.2140	5.76
B	0.659 3 (8)	0.161 0 (3)	0.425 5 (5)	H(26)	−0.0431	−0.0834	0.3123	7.34
C(11)	0.588 9 (7)	0.163 3 (2)	0.527 0 (5)	H(27)	0.1110	−0.0748	0.3365	7.34
C(12)	0.457 8 (8)	0.144 7 (3)	0.541 3 (5)	H(28)	0.0038	−0.0338	0.3690	7.34
C(13)	0.390 1 (7)	0.149 7 (3)	0.622 9 (5)	H(29)	0.2895	−0.0135	0.3282	6.22
C(14)	0.456 1 (9)	0.173 0 (3)	0.696 6 (5)	H(30)	0.3550	0.0272	0.2622	6.22
C(15)	0.587 9 (8)	0.191 2 (3)	0.687 8 (5)	H(31)	0.4265	−0.0592	0.2254	7.25
C(16)	0.653 7 (7)	0.186 3 (3)	0.605 2 (5)	H(32)	0.2752	−0.0765	0.2094	7.25
C(21)	0.824 2 (7)	0.174 7 (3)	0.440 1 (4)	H(33)	0.3408	−0.0358	0.1434	7.25
C(22)	0.916 2 (8)	0.138 3 (3)	0.476 3 (4)	H(12b)	0.4060	0.1257	0.4907	4.42
C(23)	1.052 9 (8)	0.148 4 (3)	0.496 2 (4)	H(13b)	0.2942	0.1375	0.6299	4.56
C(24)	1.104 1 (7)	0.198 0 (4)	0.477 0 (5)	H(14b)	0.4100	0.1767	0.7560	4.25
C(25)	1.019 3 (9)	0.236 7 (3)	0.438 6 (5)	H(15b)	0.6376	0.2073	0.7421	3.93
C(26)	0.881 4 (7)	0.224 9 (3)	0.421 4 (4)	H(16b)	0.7495	0.2004	0.6013	3.93
C(31)	0.649 3 (6)	0.099 9 (3)	0.383 8 (5)	H(22b)	0.8848	0.1018	0.4885	4.08
C(32)	0.663 6 (7)	0.087 8 (3)	0.290 6 (5)	H(23b)	1.1140	0.1208	0.5244	4.01
C(33)	0.672 0 (8)	0.036 5 (4)	0.258 4 (5)	H(24b)	1.2015	0.2066	0.4894	4.14
C(34)	0.665 8 (9)	−0.006 3 (4)	0.316 4 (7)	H(25b)	1.0593	0.2721	0.4242	4.27
C(35)	0.647 3 (9)	0.003 7 (3)	0.408 2 (6)	H(26b)	0.8239	0.2533	0.3947	3.70
C(36)	0.640 0 (8)	0.055 5 (3)	0.440 4 (5)	H(32b)	0.6670	0.1182	0.2456	4.48
C(41)	0.586 2 (8)	0.206 1 (3)	0.358 5 (5)	H(33b)	0.6820	0.0317	0.1902	5.24
C(42)	0.473 2 (8)	0.236 5 (3)	0.382 7 (5)	H(34b)	0.6733	−0.0423	0.2890	5.78
C(43)	0.417 0 (8)	0.277 0 (4)	0.326 5 (7)	H(35b)	0.6378	−0.0271	0.4467	6.17
C(44)	0.476 (1)	0.287 1 (4)	0.242 2 (8)	H(36b)	0.6298	0.0611	0.5064	5.15
C(45)	0.586 (1)	0.258 6 (4)	0.217 6 (6)	H(42b)	0.4293	0.2291	0.4448	4.67
C(46)	0.639 7 (8)	0.219 8 (3)	0.274 3 (6)	H(43b)	0.3349	0.2978	0.3482	6.35
				H(44b)	0.4306	0.3151	0.2013	5.81
				H(45b)	0.6264	0.2678	0.1584	5.46
				H(46b)	0.7191	0.1985	0.2513	4.77
				H(1)	0.2679	0.1909	0.2164	5.97
				H(2)	0.1933	0.1977	0.1214	5.97
				H(3)	0.4103	0.1365	0.1652	9.39
				H(4)	0.3959	0.1796	0.0887	9.39

[a] Standard deviations of the least significant digits are in parentheses. The hydrogen atom positions were computed geometrically based upon the positions of the atoms to which they are bound. Tetraphenylborate hydrogen atoms are encoded with the letter b and are numbered as in ref 21. [b] The hydrogen atoms were given the isotropic temperature factor of the atom to which they are bound. This is the isotropic temperature factor obtained after the last isotropic least-squares refinement.

parameters were varied; then the anion parameters. After two such cycles of refinement, the hydrogen atom positions were generated with HYGEN taking carbon–hydrogen distances as 0.95 Å. The hydrogen atoms were assigned the converged isotropic thermal parameters of the atom to which they are attached. Two further anisotropic least-squares cycles on all nonhydrogen atoms resulted in convergence with $R_F = 0.069$ and $R_{wF} = 0.056$ with an erf (expected error in a measurement of unit weight) of 1.59. A final difference Fourier map showed no peaks or depressions greater than 0.5 e/Å³ in any region. The final values of $|F_o|$ and $|F_c|$ for the 2679-reflection, 3σ-cutoff data set will appear as supplementary material.

Results and Discussion

Molecular Structure of $[Cu_2(Et_5dien)_2(C_2O_4)](BPh_4)_2$. The structure of the centrosymmetric compound $[Cu_2(Et_5dien)_2(C_2O_4)](BPh_4)_2$ (green needle form) was determined by single-crystal x-ray crystallographic techniques. The final positional and thermal parameters for all atoms are given in Tables III and IV[13] and the bond distances and angles are summarized in Table V. The oxalate bridge and first coordination sphere ligand atoms are labeled as indicated in Figure 1, whereas the ethylene carbon atoms of Et_5dien are variously labeled C(1), C(2), C(3), and C(4) and the ethyl carbon atoms of Et_5dien are identified as C(*I*), where *I* runs from 50 to 59. The carbon and hydrogen atoms of the tetraphenylborate ion are labeled as before.[21]

The compound $[Cu_2(Et_5dien)_2(C_2O_4)](BPh_4)_2$ consists of discrete $[Cu_2(Et_5dien)_2(C_2O_4)]^{2+}$ and BPh_4^- units. The latter isolate the dimeric Cu(II) cations such that the shortest *inter*dimer Cu–Cu distance is 12.638 (1) Å. The local Cu(II) ion environments and the oxalate bridging group in the dimeric

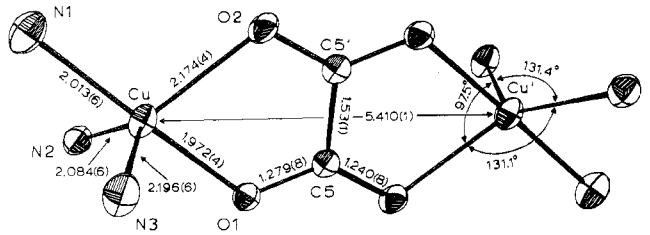

Figure 1. ORTEP plotting of the inner coordination sphere and oxalate bridge of $[Cu_2(Et_5dien)_2(C_2O_4)]^{2+}$ showing all bond distances and the three bond angles in the trigonal plane. The dimer is located about a center of inversion.

cation are illustrated in Figure 1. As can be seen, the dimeric cation consists of two Cu(II) ions, separated by 5.410 (1) Å and bridged by a bis-bidentate oxalate ion. At each Cu(II) ion, an Et_5dien ligand forms two five-membered chelate rings and, apparently, enforces a distorted TBP geometry. The single secondary nitrogen atom, N(1), of the Et_5dien ligand occupies an axial coordination site, whereas the two primary nitrogen atoms, N(2) and N(3), take equatorial sites. The remaining two Cu(II) TBP coordination sites are occupied by two oxalate oxygen atoms, with O(1) in the other axial site while O(2) completes the equatorial plane. The equatorial plane, therefore, is comprised of atoms O(2), N(2), and N(3) with the Cu(II) ion only 0.0045 (8) Å out of this plane. The approximate trigonal axis of each Cu(II) ion is slightly bent with N(1)–Cu–O(1) = 177.5 (2)°. In addition, it can be seen in Figure 1 that the three bond angles in the trigonal plane deviate appreciably from the 120° value expected for TBP geometry. All of these distortions from the idealized TBP geometry reflect the limitations placed upon the molecule by the bite of the oxalate bridge in combination with the steric interactions of the backside triamine ligand, Et_5dien. A stereoscopic view of $[Cu_2(Et_5dien)_2(C_2O_4)]^{2+}$ is given in Figure 2 and this gives the best opportunity to see the Cu(II) coordination geometry.

Whereas the ligand dien tends to complex metal ions such that the two terminal nitrogen atoms are trans to each other,[22-25] it has been noted[26] that alkylation imposes steric constraints which lead to a folding of the ligand so as to occupy three cis coordination sites. Thus, in changing from dien to an alkylated dien, the geometry of a five-coordinate Cu(II) complex would tend to change from SP to TBP. In both $[Cu_2(Et_5dien)_2(C_2O_4)]^{2+}$ and $Cu(Et_4dien)(N_3)Br$,[10] the coordination is clearly TBP with the unique (secondary) nitrogen atom occupying one axial site. Recent crystallographic investigations of $[Cu_2(Me_5dien)_2(N_3)_2](BPh_4)_2$[12] and $[Cu_2(Me_5dien)_2(CA)](BPh_4)_2$,[27] where CA is the dianion of chloranilic acid, have shown that the Cu(II) coordination geometry is intermediate between TBP and SP. The monomeric compounds $Co(Me_5dien)Cl_2$[28] and $Co(Et_4dien)Cl_2$[26] also appear to adopt an intermediate geometry.

Attention should be drawn to the bond lengths summarized in Figure 1 for $[Cu_2(Et_5dien)_2(C_2O_4)]^{2+}$. The three Cu–N bond lengths fall within the range observed for Cu^{II}–dien complexes. The shortest Cu–N bond length (2.013 Å) is associated with the apical secondary nitrogen atom, and this is also the case in $Cu(Et_4dien)(N_3)Br$. However, in several other TBP Cu(II) complexes, e.g., [Cu(bpy)I]I,[29a] [Cu(tren)(NCS)](SCN),[29b] [Cu(1,7-bis(2-pyridyl)-2,6-diazaheptane)(NCS)](SCN),[29c] and $[Cu_2(tren)_2X_2](BPh_4)_2$ (X^- = CN^-,[21] NCO^-,[29d] NCS^-,[29d] Cl^- [29d]), there is very little difference in the axial and equatorial Cu–N bond lengths. The short Cu–N bond length for the secondary nitrogen atom in $[Cu_2(Et_5dien)_2(C_2O_4)]^{2+}$ is most likely a result of the steric characteristics of the Et_5dien ligand. All other dimensions in the ligand Et_5dien seem normal, except for N(2)–C(52)–C(53) (=128 (1)°) which could result from contacts between C(53)

Table V. Molecular Distances (Å) and Angles (deg) for $[Cu_2(Et_5dien)_2(C_2O_4)](BPh_4)_2$[a]

Distances within $[Cu_2(Et_5dien)_2(C_2O_4)]^{2+}$			
Cu-Cu'	5.410 (1)	N(2)-C(2)	1.45 (1)
Cu-O(1)	1.972 (4)	N(3)-C(4)	1.47 (1)
Cu-O(2)	2.174 (4)	C(1)-C(2)	1.38 (2)
Cu-N(1)	2.013 (6)	C(3)-C(4)	1.47 (1)
Cu-N(2)	2.084 (6)	N(2)-C(52)	1.43 (1)
Cu-N(3)	2.196 (6)	C(52)-C(53)	1.33 (2)
O(1)-C(5)	1.279 (8)	N(2)-C(54)	1.45 (1)
O(2)'-C(5)	1.240 (8)	C(54)-C(55)	1.50 (1)
C(5)-C(5)'	1.53 (1)	N(3)-C(56)	1.46 (1)
N(1)-C(1)	1.47 (1)	C(56)-C(57)	1.51 (1)
N(1)-C(3)	1.50 (1)	N(3)-C(58)	1.48 (1)
N(1)-C(50)	1.49 (1)	C(58)-C(59)	1.49 (1)
C(50)-C(51)	1.49 (1)		
Angles within $[Cu_2(Et_5dien)_2(C_2O_4)]^{2+}$			
O(1)-Cu-O(2)	80.2 (2)	O(1)-C(5)-C(5)'	116.1 (6)
O(1)-Cu-N(1)	177.5 (2)	O(2)-C(5)'-C(5)	118.3 (6)
O(1)-Cu-N(2)	92.8 (2)	O(1)-C(5)-O(2)'	125.7 (6)
O(1)-Cu-N(3)	95.6 (2)	C(1)-N(1)-C(50)	111.7 (6)
O(2)-Cu-N(1)	98.8 (2)	C(1)-N(1)-C(3)	107.2 (6)
O(2)-Cu-N(2)	131.1 (2)	C(3)-N(1)-C(50)	108.9 (6)
O(2)-Cu-N(3)	97.5 (2)	N(1)-C(1)-C(2)	114.1 (8)
N(1)-Cu-N(2)	86.1 (2)	N(1)-C(3)-C(4)	111.6 (7)
N(1)-Cu-N(3)	86.8 (3)	N(1)-C(50)-C(51)	116.4 (7)
N(2)-Cu-N(3)	131.4 (2)	C(1)-C(2)-N(2)	119.0 (9)
Cu-O(1)-C(5)	115.9 (4)	C(2)-N(2)-C(52)	108.4 (8)
Cu-O(2)-C(5)'	109.5 (4)	C(2)-N(2)-C(54)	106.2 (7)
Cu-N(1)-C(1)	108.7 (5)	C(52)-N(2)-C(54)	112.1 (7)
Cu-N(1)-C(3)	104.6 (5)	N(2)-C(52)-C(53)	128 (1)
Cu-N(1)-C(50)	115.2 (5)	N(2)-C(54)-C(55)	117.9 (7)
Cu-N(2)-C(2)	103.1 (6)	C(3)-C(4)-N(3)	112.4 (8)
Cu-N(2)-C(52)	115.9 (6)	C(4)-N(3)-C(56)	108.6 (6)
Cu-N(2)-C(54)	110.3 (5)	C(56)-N(3)-C(58)	111.7 (6)
Cu-N(3)-C(4)	101.6 (5)	C(4)-N(3)-C(58)	108.8 (7)
Cu-N(3)-C(56)	112.7 (5)	N(3)-C(56)-C(57)	117.8 (7)
Cu-N(3)-C(58)	112.8 (5)	N(3)-C(58)-C(59)	114.8 (8)
Bond Distances in Tetraphenylborate Anion			
C(11)-C(12)	1.38 (1)	C(31)-C(32)	1.40 (1)
C(12)-C(13)	1.38 (1)	C(32)-C(33)	1.37 (1)
C(13)-C(14)	1.36 (1)	C(33)-C(34)	1.36 (1)
C(14)-C(15)	1.38 (1)	C(34)-C(35)	1.38 (1)
C(15)-C(16)	1.39 (1)	C(35)-C(36)	1.38 (1)
C(16)-C(11)	1.41 (1)	C(36)-C(31)	1.39 (1)
C(21)-C(22)	1.37 (1)	C(41)-C(42)	1.40 (1)
C(22)-C(23)	1.38 (1)	C(42)-C(43)	1.40 (1)
C(23)-C(24)	1.37 (1)	C(43)-C(44)	1.39 (2)
C(24)-C(25)	1.38 (1)	C(44)-C(45)	1.35 (2)
C(25)-C(26)	1.40 (1)	C(45)-C(46)	1.37 (1)
C(26)-C(21)	1.40 (1)	C(46)-C(41)	1.39 (1)
B-C(11)	1.65 (1)	B-C(31)	1.65 (1)
B-C(21)	1.66 (1)	B-C(41)	1.64 (1)
Bond Angles in the Tetraphenylborate Anion			
C(12)-C(11)-C(16)	114.2 (6)	C(32)-C(31)-C(36)	114.4 (6)
C(13)-C(12)-C(11)	124.7 (7)	C(33)-C(32)-C(31)	122.8 (7)
C(14)-C(13)-C(12)	119.1 (7)	C(34)-C(33)-C(32)	121.3 (8)
C(15)-C(14)-C(13)	119.3 (7)	C(35)-C(34)-C(33)	117.8 (8)
C(16)-C(15)-C(14)	120.9 (7)	C(36)-C(35)-C(34)	120.7 (8)
C(11)-C(16)-C(15)	121.9 (6)	C(31)-C(36)-C(35)	122.9 (7)
C(22)-C(21)-C(26)	114.0 (6)	C(42)-C(41)-C(46)	114.2 (7)
C(23)-C(22)-C(21)	125.2 (7)	C(43)-C(42)-C(41)	123.0 (7)
C(24)-C(23)-C(22)	118.6 (7)	C(44)-C(43)-C(42)	118.6 (9)
C(25)-C(24)-C(23)	120.0 (7)	C(45)-C(44)-C(43)	120 (1)
C(26)-C(25)-C(24)	119.2 (7)	C(46)-C(45)-C(44)	120.5 (9)
C(21)-C(26)-C(25)	122.9 (7)	C(41)-C(46)-C(45)	124.0 (8)
B-C(11)-C(12)	122.5 (6)	C(11)-B-C(21)	108.1 (5)
B-C(11)-C(16)	123.2 (6)	C(11)-B-C(31)	109.9 (6)
B-C(21)-C(22)	122.4 (6)	C(11)-B-C(41)	108.7 (6)
B-C(21)-C(26)	123.5 (6)	C(21)-B-C(31)	106.6 (6)
B-C(31)-C(32)	123.4 (6)	C(21)-B-C(41)	109.8 (6)
B-C(31)-C(36)	121.9 (6)	C(31)-B-C(41)	113.6 (6)
B-C(41)-C(42)	124.0 (6)		
B-C(41)-C(46)	121.6 (6)		

[a] Estimated standard deviations of the least significant figures are given in parentheses.

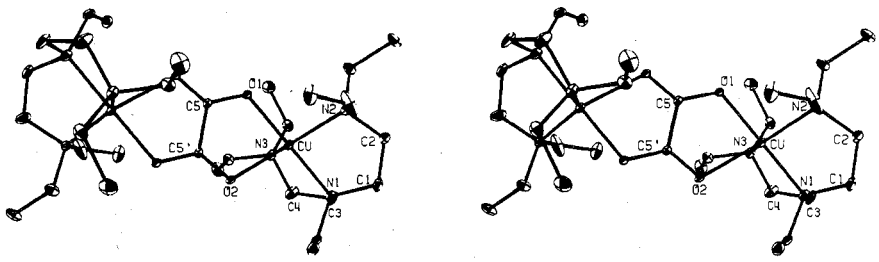

Figure 2. Stereoscopic ORTEP plotting of $[Cu_2(Et_5dien)_2(C_2O_4)]^{2+}$; the hydrogen atoms are not shown.

and the two nearby oxygen atoms.

There have been several reportings of crystal structures of copper(II) oxalates: $K_2Cu(C_2O_4)_2 \cdot 2H_2O$,[30a,b] $Cs_2Cu(C_2O_4)_2 \cdot 2H_2O$,[30c] $(NH_4)_2Cu(C_2O_4)_2 \cdot 2H_2O$,[30d] α-$Cu(NH_3)_2(C_2O_4)$,[30e] $Li_2Cu(C_2O_4)_2 \cdot 6H_2O$,[30f] Cu(dien)$(C_2O_4) \cdot 4H_2O$,[22c] $Cu(NH_3)_2(C_2O_4) \cdot 2H_2O$,[30g] $Cu(NH_3)(C_2O_4)$,[30h] $[Cu_2(dien)_2(C_2O_4)](ClO_4)_2$,[11] and Cu$(Me_2en)(C_2O_4) \cdot H_2O$.[30i] In the cases where oxalate functions as a bridge between two Cu(II) ions, it may occupy either two equatorial sites[30g,i] or one axial and one equatorial.[11,30a,b,e,h] It is interesting to note that in all compounds, *except* for $[Cu_2(Et_5dien)_2(C_2O_4)](BPh_4)_2$, whenever the axial site could be distinguished from the equatorial position, the equatorial bond is always the shorter of the two Cu–O bonds. Furthermore, in the above compounds, the Cu–O(eq) bond lengths range from 1.96 to 2.02 Å, while the Cu–O(ax) range is 2.23–2.48 Å. In $[Cu_2(Et_5dien)_2(C_2O_4)](BPh_4)_2$ the corresponding distances are 2.174 (4) and 1.972 (4) Å, respectively. The former is somewhat larger than the equatorial bond length range, but certainly the most amazing bond length is the axial Cu–O distance of 1.972 (4) Å which is considerably shorter than the axial range. The fixed bite of the oxalate bridge and the bulkiness of the Et_5dien ligand are the probable causes of this.

The molecular dimensions of the oxalate group are relatively invariant in all Cu(II) oxalate complexes. The oxalate C–C bond, 1.53 (1) Å, of $[Cu_2(Et_5dien)_2(C_2O_4)](BPh_4)_2$ is among the shortest reported for any copper(II) oxalate compound; however, there is only a small overall variation in this length (1.53–1.65 Å). The oxalate dianion is planar, a common feature of Cu(II) oxalate compounds, despite the presence of what appears to be a C–C single bond. The O–C–O angle of 125.7 (6)° falls within the normal range for the oxalate dianion.[30,31]

The BPh_4^- anion has typical bond distances and angles. All four phenyl groups are planar; the least-squares planes can be found in Table VI.[13] The mean B–C bond distance is 1.65 (1) Å and the mean C–C distance is 1.38 (1) Å. The bond angles within each phenyl group are found in the range of 120 ± 6.0°, indicating the presence of some distortion. In all phenyl rings C(2)–C(1)–C(6) is the smallest (mean is 114.3 (6)°), whereas the ring angle centered at the ortho carbon atom is the largest angle (mean 123.4 (7)°). These results are in accord with our previous crystallographic work[21,29d] on BPh_4^- compounds which also indicates some amount of crowding about the boron atom. Similar results have been reported for CPh_4,[32] $SiPh_4$,[33] and $GePh_4$,[34] whereas the $AsPh_4^+$ species in $Ph_4As[FeCl_4]$ has recently been shown[35] to have nondistorted C–C–C angles within the phenyl rings.

Oxalate-Bridged BPh_4^- Complexes. Previously we reported variable-temperature magnetic susceptibility and EPR data for $[Cu_2(dien)_2(C_2O_4)](BPh_4)_2$.[8] Tables VII–X[13] give the variable-temperature magnetic susceptibility data for the other compounds in the series $[Cu_2("dien")_2(C_2O_4)](BPh_4)_2$ where "dien" is variously dien, dpt, Me_5dien, or Et_5dien.

As indicated in the Experimental Section, there are two crystalline forms of $[Cu_2(Et_5dien)_2(C_2O_4)](BPh_4)_2$: one is green and the other is blue. The magnetic susceptibility data

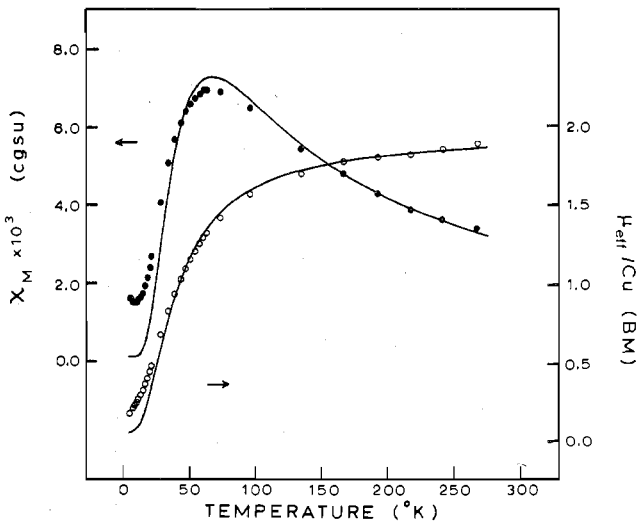

Figure 3. Experimental molar paramagnetic susceptibility (●) per dimer and effective magnetic moment (○) per Cu(II) ion vs. temperature for $[Cu_2(Et_5dien)_2(C_2O_4)](BPh_4)_2$. The solid curves represent the least-squares fit to eq 1.

for the green form are displayed in Figure 3 where it can be seen that this compound exhibits an unusually large antiferromagnetic exchange interaction for a Cu(II) dimer with such an extended bridging group. There is a peak in the susceptibility at 60 K and the effective magnetic moment per Cu(II) ion varies from 1.90 μ_B at 267 K to 0.16 μ_B at 4.2 K. The susceptibility data for this compound were least-squares fit to the Bleaney–Bowers equation for isotropic exchange in a Cu(II) dimer

$$\chi_M = \frac{Ng^2\beta^2}{kT}\left[\frac{2}{3 + \exp(-2J/kT)}\right] + N\alpha \qquad (1)$$

The temperature-independent paramagnetism, $N\alpha$, for a Cu(II) dimer was taken as 120×10^{-6} cgsu/mol of dimer. Generally, in the least-squares fitting, it is best to use the average g value obtained from EPR measurements, and this is the procedure that we followed for most of the compounds. When g and $N\alpha$ are fixed, there is only one fitting parameter for each compound, the exchange parameter J. It was found that in order to obtain a satisfactory fit to the magnetic data for green $[Cu_2(Et_5dien)_2(C_2O_4)](BPh_4)_2$ the average g value had to be adjusted to 2.26 to fit the high-temperature data. With the g value fixed at 2.26, least-squares fitting of the data gave a J value of -37 cm^{-1}. In Figure 3 this least-squares fitting is represented by lines, which can be seen to fit the data reasonably well. The deviation of observed and theoretical susceptibility data at the lowest temperature is most probably due to a small amount (ca. 0.2%) of a paramagnetic Cu(II) monomer. In a latter section the exchange mechanism will be discussed for the series of copper(II) oxalate dimers.

It was of interest to see whether the *blue* crystalline form of $[Cu_2(Et_5dien)_2(C_2O_4)](BPh_4)_2$ exhibited the same mag-

Table XI. Summary of Magnetic Susceptibility and EPR Parameters for Oxalate-, Squarate-, Succinate-, and Cyanate-Bridged Copper(II) Dimers

Compd	J, cm^{-1}	SE[a]	$\bar{g}$[b]	g_1[c]	g_2	g_3	Other features[d]
$[Cu_2(Et_5dien)_2(C_2O_4)](BPh_4)_2$ (green form)	−37.4	0.1092	2.26[e] (2.127)	2.020	2.119	2.242	$\Delta M_S = 2$ (X band) with 5 visible Cu hf
$[Cu_2(Et_5dien)_2(C_2O_4)](BPh_4)_2$ (blue form)	−31.4	0.1213	2.26[e] (2.127)	2.020	2.111	2.251	$\Delta M_S = 2$ (X band) with 5 Cu hf; derivative at 2.058
$[Cu_2(Me_5dien)_2(C_2O_4)](BPh_4)_2$	−3.4	0.0305	2.111	2.037	2.061	2.235	9 Cu hf on $g_\parallel$; $\Delta M_S = 2$ (X band) shows 7 Cu hf
$[Cu_2(dpt)_2(C_2O_4)](BPh_4)_2$	−5.7	0.0261	2.114	2.032	2.074	2.236	$\Delta M_S = 2$ (X band)
$[Cu_2(dien)_2(C_2O_4)](BPh_4)_2$[f]	−7.3	0.0233	2.125	2.034	2.090	2.250	8 Cu hf on $g_\parallel$; $\Delta M_S = 2$ (X band) shows 7 Cu hf
$[Cu_2(Et_5dien)_2(C_2O_4)](ClO_4)_2$	−9.8	0.0347	2.121	2.044	2.086	2.235	$\Delta M_S = 2$ (X band) with 6 Cu hf
$[Cu_2(Me_5dien)_2(C_2O_4)](ClO_4)_2$	−2.2	0.0145	2.110	2.047	2.057	2.225	
$[Cu_2(dpt)_2(C_2O_4)](ClO_4)_2$	<∼0.5[g]		2.116	2.061	2.143	2.143	
$[Cu_2(dien)_2(C_2O_4)](ClO_4)_2$[h]	<∼0.5[g]		2.145	2.079	2.142	2.213	
$[Cu_2(Et_5dien)_2(C_2O_4)](PF_6)_2$	−9.6	0.0261	2.122	2.041	2.096	2.229	$\Delta M_S = 2$ (X band)
$[Cu_2(Me_5dien)_2(C_2O_4)](PF_6)_2$	<∼0.5[g]		2.111	2.045	2.062	2.225	
$[Cu_2(dpt)_2(C_2O_4)](PF_6)_2$	<∼0.5[g]		2.123	2.059	2.155	2.155	Very weak $\Delta M_S = 2$ (X band)
$[Cu_2(dien)_2(C_2O_4)](PF_6)_2$	<∼0.5[g]		2.122	2.074	2.074	2.217	
$[Cu_2(tren)_2(C_2O_4)](BPh_4)_2$[h]	<∼0.5[g]		2.136	2.040	2.115	2.253	$\Delta M_S = 2$ (X band)
$[Cu_2(Et_5dien)_2(C_4O_4)](BPh_4)_2$	−2.1	0.0148	2.145	2.048	2.127	2.260	$\Delta M_S = 2$ (X band)
$[Cu_2(Et_5dien)_2(O_2CCH_2CH_2CO_2)](BPh_4)_2$	<∼0.5[g]		2.114	2.029	2.087	2.227	$\Delta M_S = 2$ (X band)
$[Cu_2(Me_5dien)_2(O_2CCH_2CH_2CO_2)](BPh_4)_2$	<∼0.5[g]		2.112	2.029	2.089	2.219	$\Delta M_S = 2$ (X band)
$[Cu_2(Me_5dien)_2(NCO)_2](BPh_4)_2$	<∼0.5[g]		2.097	2.029	2.043	2.219	10 Cu hf on $g_\parallel$; $\Delta M_S = 2$ (X band) shows 7 Cu hf

[a] Standard error (SE) given by $SE = \{\sum_{i=1}^{NP} [\mu_{eff}(obsd)_i - \mu_{eff}(calcd)_i]^2/(NP - k)\}^{1/2}$, where k is the number of variable parameters used to fit the NP data points (see A. P. Ginsberg, R. L. Martin, R. W. Brookes, and R. C. Sherwood, *Inorg. Chem.*, 11, 2884 (1972)). [b] Average g values used in the magnetic susceptibility fitting obtained from Q-band EPR powder spectra except as noted. [c] g values from Q-band EPR powder spectra at ∼300 K. [d] hf = hyperfine. [e] Adjusted $\bar{g}$ values for use in magnetic susceptibility fitting; numbers in parentheses are from EPR. [f] Reference 8. [g] In these cases there are no signs of an exchange interaction in the susceptibility down to 4.2 K and so $|J| < \sim 0.5$ cm^{-1}. [h] Reference 9.

nitude of antiferromagnetic exchange. Table VIII[13] lists the data, which are very similar to those for the *green* form. In the case of the blue compound, μ_{eff} ranges from 1.95 μ_B at 270 K to only 0.09 μ_B at 4.2 K. The maximum in the susceptibility is broader for the blue compound and is centered at 53 K. Again it was necessary to fix $\bar{g}$ as 2.26 in order to get the best least-squares fitting of the data. The J value was found to be −31 cm^{-1}.

X-Band and Q-band EPR spectra have been recorded for all of the compounds in this study. The magnetic susceptibility and EPR results are summarized in Table XI. The ∼110-K Q-band EPR spectrum of a powdered sample of the green form of $[Cu_2(Et_5dien)_2(C_2O_4)](BPh_4)_2$ is shown in Figure 4, tracing B. There are two points of interest. First, the high-field signal at $g = 2.020$ is indicative of a d_{z^2} ground state,[36] which is in agreement with the TBP geometry found in the structural work. Second, the spectrum is very nonaxial with the other two g values at 2.119 and 2.242 and this is a reflection of the appreciable distortion from TBP geometry. The *blue* form of $[Cu_2(Et_5dien)_2(C_2O_4)](BPh_4)_2$ shows nearly the same rhombic powder EPR spectrum with $g_1 = 2.020$, $g_2 = 2.111$, and $g_3 = 2.251$, except that an additional weak inflection occurs between g_1 and g_2 at a g value of 2.058. The X-band spectra of both forms exhibit a single slightly asymmetric derivative at $g = 2.13$ (average g value in the Q-band spectrum is 2.127). The X-band spectra also show $\Delta M_S = 2$ transitions (1600 G) with relative intensities that are ∼0.01 times those of the $\Delta M_S = 1$ transitions. At least four copper hyperfine lines with a spacing of ∼59 G are visible on the $\Delta M_S = 2$ resonances.

The IR spectra of the blue and green forms of $[Cu_2(Et_5dien)_2(C_2O_4)](BPh_4)_2$ are essentially superimposable. This taken together with the close similarity of susceptibility and EPR data indicates that the $[Cu_2(Et_5dien)_2(C_2O_4)]^{2+}$ units in the two crystalline forms are essentially identical. Perhaps there are two packing arrangements (i.e., space groups) that are close in energy.

The magnetic susceptibility data for $[Cu_2(Me_5dien)_2(C_2O_4)](BPh_4)_2$ are displayed in Figure 5 (also Table IX[13]).

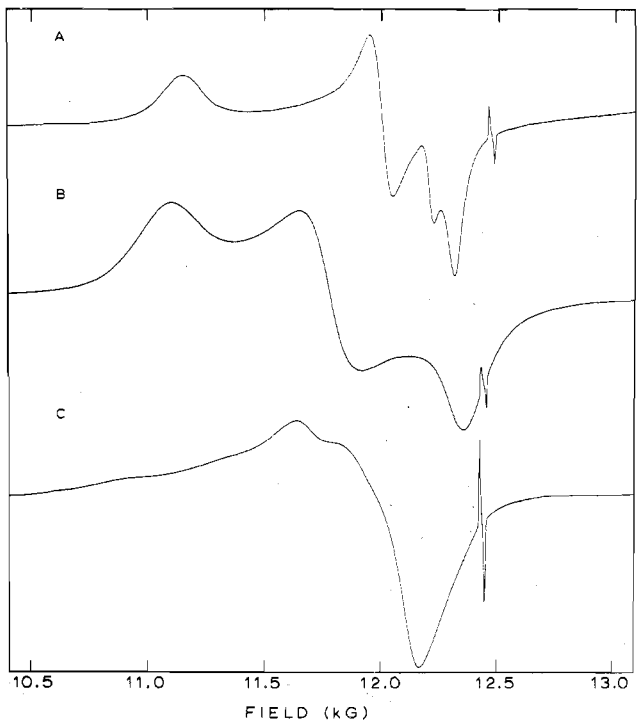

Figure 4. Q-Band (∼35 GHz) EPR spectra of powdered samples of $[Cu_2(Et_5dien)_2(C_2O_4)](ClO_4)_2$ (A), $[Cu_2(Et_5dien)_2(C_2O_4)](BPh_4)_2$ (B), and $[Cu_2(Et_5dien)_2(C_4O_4)](BPh_4)_2$ (C) recorded at ∼110 °K. The DPPH ($g = 2.0036$) resonances around 12 480 G were used to calibrate the frequency. Variations in the frequency used for the three spectra cause the DPPH signal to occur at different field positions.

An antiferromagnetic exchange interaction is evident with a susceptibility maximum (Néel temperature, T_N) at ∼6 K. The μ_{eff} per Cu(II) ion decreases gradually from 1.82 μ_B at 267 K down to 20 K, whereupon the rate of decrease increases to give 1.05 μ_B at 4.2 K. With $\bar{g}$ fixed as 2.111 from the Q-band spectrum, least-squares fitting to eq 1 gives a J value of −3.4

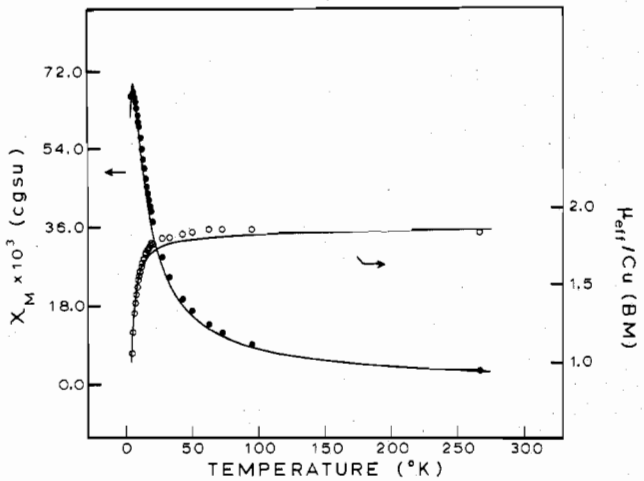

Figure 5. Experimental molar paramagnetic susceptibility (●) per dimer and effective magnetic moment (○) per Cu(II) ion vs. temperature for $[Cu_2(Me_5dien)_2(C_2O_4)](BPh_4)_2$. The lines represent the least-squares fit to eq 1.

cm^{-1}. Thus, the antiferromagnetic interaction in this compound is about one-tenth that found for $[Cu_2(Et_5dien)_2(C_2O_4)](BPh_4)_2$. Before the EPR results for $[Cu_2(Me_5dien)_2(C_2O_4)](BPh_4)_2$ are presented, we shall briefly review a few of the factors[37] which can influence the EPR of Cu(II) dimers.

Dimeric Cu(II) complexes with tetraphenylborate counterions are unique in that a substantial degree of magnetic dilution *between* dimers is possible in the *pure* solid. Interdimer distances greater than ~10 Å have allowed, in some cases,[8] the observation of zero-field split features and Cu(II) hyperfine interaction in the X- and Q-band spectra. If we consider the case where the exchange parameter J is large relative to the copper hyperfine interaction and relative to the zero-field splitting in the dimer, then we are only concerned with EPR transitions within the Cu(II) dimer triplet state. Assuming that there is only axial zero-field splitting (i.e., $D\hat{S}_z^2 \neq 0$) for the dimer, the triplet state will then be split in zero field into two levels, $|1\ 0\rangle$ and $|1\ \pm1\rangle$. Zero-field splitting in the triplet state can arise from two effects: dipole–dipole interactions between the two Cu(II) ions and spin–orbit interactions of the triplet state with excited states. The latter is called the pseudodipolar zero-field interaction and is generally neglected when the exchange interaction is such that $|J| < \sim 30\ cm^{-1}$.[37] We will assume that this is the case. The interion dipolar zero-field splitting (D_{dd}) in the triplet state is given by

$$D_{dd} = (3/4)g^2\beta^2\left\langle \frac{1 - 3\cos^2\theta}{r^3} \right\rangle \qquad (2)$$

where θ is the angle between the Cu–Cu vector and the magnetic field, r is taken as the intradimer Cu–Cu distance, and the angular brackets indicate an average value. Equation 2 shows that the dipolar zero-field splitting of the triplet state can be different for different magnetic field orientations. In other words, the dipolar splitting seen for the ($\Delta M_S = 1$) $g_\parallel$ signal will not generally be equal to that seen for the ($\Delta M_S = 1$) $g_\perp$ signal. It is also evident that, when $\theta \simeq 54°$ for a particular resonance, that signal will show no zero-field splitting.

In summary, an idealized spectrum for a Cu(II) dimer with axial symmetry (and with above assumptions) would consist of two $\Delta M_S = 1$ features: a $g_\parallel$ feature which is zero-field split into two resonances and a $g_\perp$ feature which is zero-field split into two resonances. Generally each of the two $g_\parallel$ resonances will exhibit seven-line copper hyperfine patterns. If the $g_\parallel$ zero-field splitting is small, the two seven-line patterns can overlap. The $g_\parallel$ signal can, thus, consist of 7–14 lines, depending on the size of the zero-field splitting. The magnitude of zero-field splitting is not dependent on the EPR microwave frequency that is used.

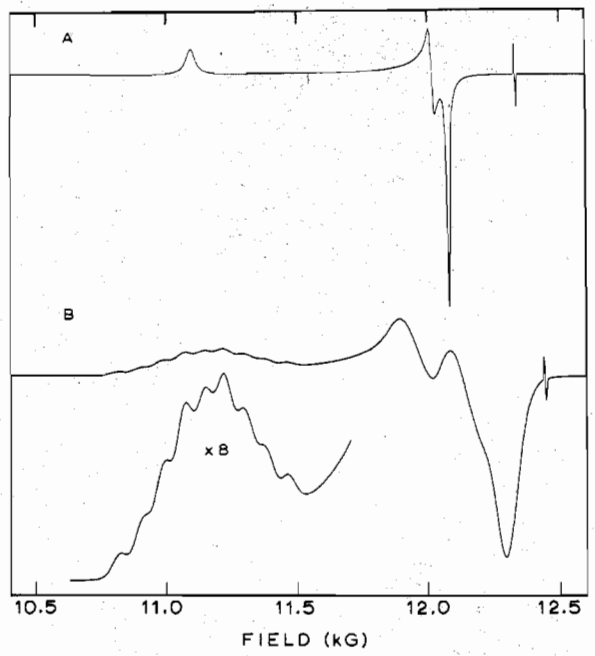

Figure 6. Q-Band (~35 GHz) EPR spectra of powdered samples of $[Cu_2(Me_5dien)_2(C_2O_4)](ClO_4)_2$ (A) and $[Cu_2(Me_5dien)_2(C_2O_4)](BPh_4)_2$ (B) at ~110 K with DPPH as a frequency calibrant.

At "half-field" (~1500 G for an X-band spectrum) there is a formally forbidden transition with $\Delta M_S = 2$. This transition is between the $|1\ -1\rangle$ and $|1\ 1\rangle$ triplet levels and to first order does not depend on D_{dd}. Thus, the $\Delta M_S = 2$ resonance for our Cu(II) dimer does *not* show any zero-field splitting. It should be noted, however, that the intensity of the $\Delta M_S = 2$ transition does depend in second order on the zero-field splitting. It is sufficient for our purposes to know that the $\Delta M_S = 2$ transition only has somewhat appreciable intensity for an axial Cu(II) dimer when the magnetic field is normal to the Cu–Cu axis and not coincidental with the x or y axis of the g tensor. In short, no zero-field splitting is seen for the $\Delta M_S = 2$ transition and an idealized spectrum for an axial dimer could consist of seven copper hyperfine lines. When the symmetry is lower than axial, the spectrum will be more complicated.[36] In practice, a $\Delta M_S = 2$ resonance is easier to see in an X-band spectrum than in a Q-band spectrum. Finally, it should be noted that in an exchange-coupled Cu(II) dimer the copper hyperfine spacing is half that of the analogous Cu(II) monomer.[38]

The Q-band EPR spectrum of a powdered sample of $[Cu_2(Me_5dien)_2(C_2O_4)](BPh_4)_2$ at ~110 K is shown in Figure 6, tracing B. The spectral features are quite close to those previously reported[8] for $[Cu_2(dien)_2(C_2O_4)](BPh_4)_2$; however, in contrast to the dien case where only eight hyperfine lines with an average value of $A_\parallel(Cu) = 81$ G are discernible, the spectrum for the Me_5dien compound clearly shows nine hyperfine lines ranging in spacing from 72 to 100 G with an average of 80 G. A pattern of nine hyperfine lines results from an overlapping of two seven-line patterns if the zero-field splitting in this g signal is equal to $2A_\parallel(Cu)$. The high-field signal also seems to be zero-field split. That is, the appearance (i.e., essentially two features) of the high-field signal does not change in going from the 110-K Q-band spectrum (Figure 6, tracing B) to the 6-K X-band spectrum. The spacing between the two nearby derivatives is ~190 G and this is probably the

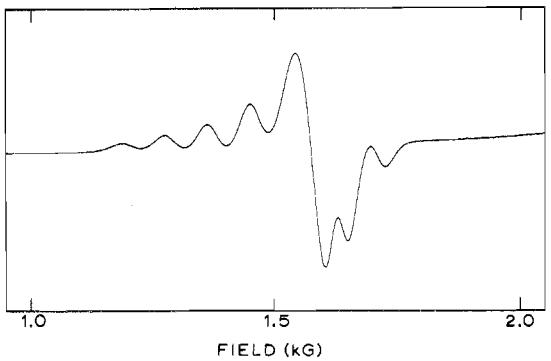

Figure 7. Low-field portion of the X-band (9.1730 GHz) EPR spectrum of powdered $[Cu_2(Me_5dien)_2(C_2O_4)](BPh_4)_2$ showing the $\Delta M_S = 2$ region recorded at ~6 K.

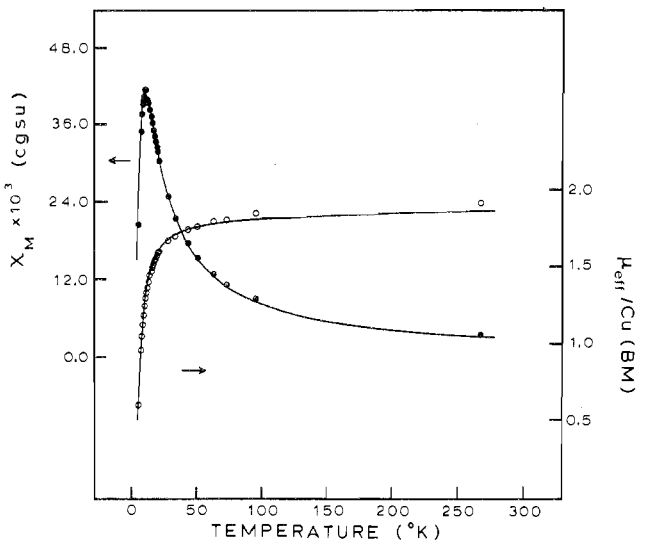

Figure 8. Experimental molar paramagnetic susceptibility (●) per dimer and effective magnetic moment (○) per Cu(II) ion vs. temperature for $[Cu_2(dpt)_2(C_2O_4)](BPh_4)_2$. The solid curves are the least-squares fit to eq 1.

zero-field splitting in the perpendicular signal. In summary, the $\Delta M_S = 1$ EPR features for $[Cu_2(Me_2dien)_2(C_2O_4)](BPh_4)_2$ clearly show that the two unpaired electrons are exchanging between the two Cu(II) ions in the μ-oxalato-bridged dimer and that, with the $g_{\|}$ signal at 2.235, the local Cu(II) coordination geometry must have a fair degree of SP character.

A $\Delta M_S = 2$ transition is observed for $[Cu_2(Me_5dien)_2(C_2O_4)](BPh_4)_2$ in the X-band spectrum. Figure 7 illustrates the $\Delta M_S = 2$ transition seen for a powdered sample maintained at 6 K. The resolution of this spectrum is unusual for an *undoped* dimeric Cu(II) compound. Seven copper hyperfine lines are clearly visible, and because this is a so-called $\Delta M_S = 2$ transition, there is no zero-field splitting. The average hyperfine spacing is 90 G. Structural work is needed before this apparently simple looking signal can be properly simulated.

The effect of alkylation of the dien ligand has been to distort the SP dien complex[39] partly (with Me_5dien) or totally (with Et_5dien) toward TBP geometry. Another type of backside ligand change is effected by lengthening the ethylene moieties of dien to the propylene linkages of dpt. The magnetic susceptibility data of $[Cu_2(dpt)_2(C_2O_4)](BPh_4)_2$ are illustrated in Figure 8 (also see Table X[13]). This compound also exhibits an antiferromagnetic exchange interaction, this time with $T_N = 10$ K, $J = -5.7$ cm^{-1}, and $g = 2.114$. The effective magnetic moment per Cu(II) ion decreases from 1.89 μ_B at 267 K to 0.58 μ_B at 4.2 K. The Q-band EPR spectrum in Figure 9 (tracing B) shows three features with g values of $g_1 = 2.032$, $g_2 = 2.074$, and $g_3 = 2.236$. These values are nearly the same

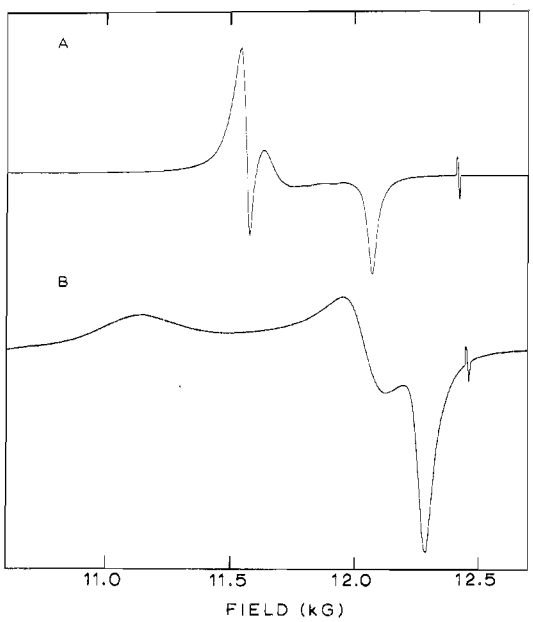

Figure 9. Q-Band (~35 GHz) EPR spectra of powdered samples of $[Cu_2(dpt)_2(C_2O_4)](ClO_4)_2$ (A) and $[Cu_2(dpt)_2(C_2O_4)](BPh_4)_2$ (B) at ~110 K with DPPH for frequency calibration.

as we observed for the Me_5dien and dien analogues. In contrast, the dpt spectrum shows no hyperfine interaction on the low-field signal. The splitting in the $\Delta M_S = 1$ region of the Q-band spectrum, unlike that of the Me_5dien analogue, is due to g value anisotropy rather than dipolar zero-field splitting, since no splitting is observable in the X-band spectrum. The EPR data indicate a Cu(II) ion geometry in $[Cu_2(dpt)_2(C_2O_4)](BPh_4)_2$ that approximates SP geometry; however, the exact distortion from this idealized geometry must be somewhat different than in $[Cu_2(Me_5dien)_2(C_2O_4)](BPh_4)_2$ as evidenced by the difference in zero-field content in the EPR spectra.

Three crystal structures are relevant to a discussion of the Cu(II) ion coordination geometry in $[Cu_2(dpt)_2(C_2O_4)](BPh_4)_2$. Structures have been reported for $Cu(dpt))(NCS)_2$,[40] $[Cu(dpt)(NCS)](ClO_4)$,[41] and $[Cu(dpt)(OAc)](ClO_4)$,[42] where OAc^- is the acetate ion. In all three compounds, the dpt ligand adopts a meridional configuration which places all three dpt nitrogen atoms in a square plane. All three Cu(II) complexes are essentially SP; there is semicoordination by a perchlorate oxygen atom in $[Cu(dpt)(NCS)](ClO_4)$ and in the third compound an oxygen atom from another Cu(II) complex bonds into the remaining axial position of the square pyramid. From the above structural data, it seems clear that the Cu(II) ion coordination geometry in $[Cu_2(dpt)_2(C_2O_4)](BPh_4)_2$ would be expected to be distorted SP.

Oxalate-Bridged Complexes. Counterion Effects. The magnetic exchange interaction in a given oxalate-bridged cation would change if the molecular dimensions of the dimer are altered. Replacing BPh_4^- by ClO_4^- or PF_6^- could modify the molecular dimensions of the dimer either by changing lattice forces (e.g., the space groups are different) or by causing the new counterion to semicoordinate to the Cu(II) ions in the dimer. Perchlorate ion does coordinate to metal ions; a particular compound in which this occurs is $[Zn_2(dpt)_2(C_2O_4)](ClO_4)_2$.[11] The effect of this weak coordination on the local geometry of the Cu(II) ion in an oxalate-bridged dimer is difficult to assess without a crystal structure, but a comparison of EPR spectrum can tell whether the ground state is very affected.

The magnetic susceptibility data for $[Cu_2(\text{"dien"})_2(C_2O_4)](ClO_4)_2$, where "dien" is Et_5dien, Me_5dien, and dpt,

are compiled in Tables XII–XIV.[13] For the Et_5dien complex, the susceptibility data show a maximum at 18 K and can be least-squares fit to a J value of -9.8 cm^{-1} with $\bar{g}$ fixed at 2.12 from the EPR spectrum. The 110-K Q-band spectrum is given in Figure 4, tracing A. The spectrum looks similar to that for the corresponding BPh_4^- salt. The better resolved signals for the ClO_4^- salt apparently bring out the "extra" feature seen at high fields. It seems that the Cu(II) ion coordination geometry is still TBP in this ClO_4^- compound. Inspection of the stereoscopic view of $[Cu_2(Et_5dien)_2(C_2O_4)]^{2+}$ in Figure 2 shows that there is little likelihood that ClO_4^- could become semicoordinated to the Cu(II) ions. However, the geometry of this cation could be somewhat different in the ClO_4^- salt than it is in the BPh_4^- salt and this could account for the reduction in antiferromagnetic interaction from $J = -37$ cm^{-1} to $J = -9.8$ cm^{-1}.

The Me_5dien–C_2O_4 dimer also shows a reduction in antiferromagnetic interaction in replacing BPh_4^- with ClO_4^-. The susceptibility data given in Table XIII[13] for $[Cu_2(Me_5dien)_2(C_2O_4)](ClO_4)_2$ fit very well to a J value of -2.2 cm^{-1} with $\bar{g}$ fixed at 2.110. Figure 6 shows a comparison of the Q-band EPR spectra of $[Cu_2(Me_5dien)_2(C_2O_4)](ClO_4)_2$ and the BPh_4^- analogue. The two most obvious differences between these two spectra are the very reduced line widths and the absence of copper hyperfine interaction on the low-field signal in the ClO_4^- spectrum. These differences, in fact, demonstrate the distinct advantage that BPh_4^- provides in obtaining additional EPR observables in undoped solids. There is most certainly an *intra*dimer exchange interaction present in $[Cu_2(Me_5dien)_2(C_2O_4)](ClO_4)_2$ with $J = -2.2$ cm^{-1}. The difference between the EPR spectra of the ClO_4^- and BPh_4^- salts results from the fact that, in the former, there is an *inter*dimer exchange interaction propagated by the ClO_4^- anion. When the *inter*dimer interaction exceeds the copper hyperfine interaction ($\sim$0.01–0.02 cm^{-1}), electrons exchange between the copper dimers. Larger interactions lead to greater exchange frequencies and these, in turn, result in a broadening of individual hyperfine lines followed by a coalescence of the hyperfine lines for each signal into a sharp single resonance at a particular g value. An electron exchanging between copper dimers will experience an average of copper nuclear hyperfine states.

The EPR spectra for $[Cu_2(Me_5dien)_2(C_2O_4)](ClO_4)_2$, as well as structural data for other Cu(II) Me_5dien complexes, show that the Cu(II) coordination geometry is that of a distorted square pyramid in which the steric interactions of the methyl groups cause a distortion from the basal plane.

Curtis previously reported[14] the preparation of $[Cu_2(dpt)_2(C_2O_4)](ClO_4)_2$, which he characterized by infrared and reflectance spectra and an μ_{eff} per Cu(II) of 1.90 μ_B. He reported that the compound is not isostructural to the TBP zinc(II) analogue. We have measured the magnetic susceptibility of $[Cu_2(dpt)_2(C_2O_4)](ClO_4)_2$ from 267 to 4.2 K; see Table XIV.[13] There is no sign of an exchange interaction throughout the temperature range with μ_{eff} per Cu(II) of 1.85 (3) μ_B, where the average deviation for all the data points is given in parentheses. The 110-K Q-band EPR spectrum is reproduced in Figure 9, tracing A, and can be compared with the spectrum for the corresponding BPh_4^- salt given as tracing B. The EPR spectra in Figure 9 reveal an appreciable change in ground-state character between the BPh_4^- and ClO_4^- compounds. The ClO_4^- spectrum is axial and it appears that $g_\parallel = 2.061$ and $g_\perp = 2.143$, so that now $g_\parallel$ is less than $g_\perp$.

Four complexes with the composition of $[Cu_2(\text{"dien"})_2(C_2O_4)](PF_6)_2$, where "dien" is either Et_5dien, Me_5dien, dpt, or dien, were prepared in order to further characterize the nature of the counterion dependence of the magnetic properties. Table XI summarizes the magnetic susceptibility and

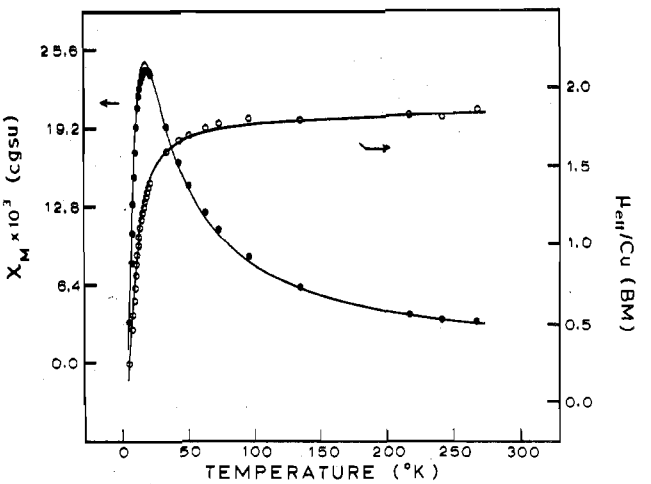

Figure 10. Experimental molar paramagnetic susceptibility (●) per dimer and effective magnetic moment (○) per Cu(II) ion vs. temperature for $[Cu_2(Et_5dien)_2(C_2O_4)](PF_6)_2$. The solid curves result from least-squares fitting to eq 1.

EPR data for the four PF_6^- compounds (see Tables XV[13] and XVI[13] for the data). As might be anticipated from the relative sizes of ClO_4^- and PF_6^- compared to BPh_4^-, the data for the PF_6^- compounds are very similar to those for the ClO_4^- compounds. Only $[Cu_2(Et_5dien)_2(C_2O_4)](PF_6)_2$ shows an antiferromagnetic interaction with a J value of -9.6 cm^{-1}. Figure 10 shows that the data for this compound are nicely fit to eq 1. There are no signs of a measurable exchange interaction down to 4.2 K for the other three PF_6^- compounds where the average μ_{eff} values are 1.83 (3), 1.90 (3), and 1.89 (4) μ_B, respectively.

Three limiting structures summarize the possible μ-oxalatocopper(II) dimers with triamine ligands:

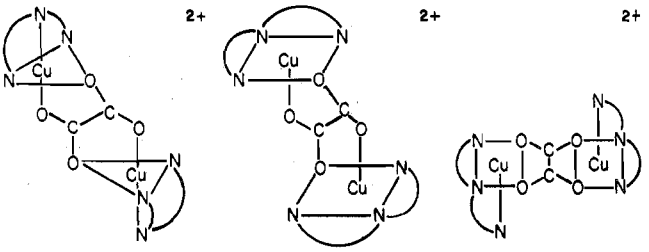

I II III

From our x-ray work we know that the compound $[Cu_2(Et_5dien)_2(C_2O_4)](BPh_4)_2$ has distorted TBP Cu(II) coordination geometries as sketched for structure I. From our EPR measurements we conclude that all three salts of $[Cu_2(Et_5dien)_2(C_2O_4)]^{2+}$ have Cu(II) geometries approaching structure I. There is probably some difference in distortion (e.g., trigonal-plane angles, etc.) from TBP geometry between the BPh_4^- compound on the one hand and the ClO_4^- and PF_6^- compounds on the other. The Cu(II) dimer in $[Cu_2(dien)_2(C_2O_4)](ClO_4)_2$ has been shown by x-ray work[11] to approximate to structure II. Our x-ray work on $[Cu_2(Me_5dien)_2(N_3)_2](BPh_4)_2$[12] and $[Cu_2(Me_5dien)_2(CA)](BPh_4)_2$[27] shows that, when a careful analysis of molecular dimensions is made, the geometries of the Cu(II) dimers in these two compounds are closest to structure II but are somewhat distorted toward structure III. From the above structural work and the various EPR spectra, we conclude that complexes of the form $[Cu_2(\text{"dien"})_2(C_2O_4)]X_2$, where "dien" is Me_5dien or dien and X^- is ClO_4^- or PF_6^-, resemble structure II. Also, complexes of the form $[Cu_2(\text{"dien"})_2(C_2O_4)](BPh_4)_2$, where "dien" is Me_5dien, dpt, or dien, have a structure that is a combination of structures II and III. Because of the somewhat peculiar EPR pattern given in Figure 9, tracing A,

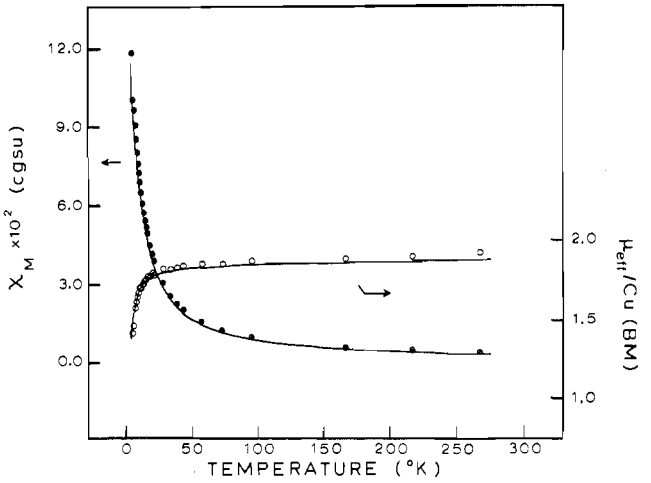

Figure 11. Experimental paramagnetic susceptibility (●) per dimer and effective magnetic moment (○) per Cu(II) ion vs. temperature for $[Cu_2(Et_5dien)_2(C_4O_4)](BPh_4)_2$ using eq 1 to generate the least-squares fit solid curves.

we are least sure of the geometry of the Cu(II) dimers in the ClO_4^- and PF_6^- salts with dpt.

Squarate-, Succinate-, and Cyanate-Bridged Complexes. It is possible to gain some insight into the mechanism of exchange interaction operative in an oxalate-bridged Cu(II) dimer by studying complexes wherein everything is kept constant except the oxalate bridge is replaced by an analogous bridge. In an earlier paper[6] we presented susceptibility data ($J = -17$ cm^{-1}) for a particular nickel(II) oxalate dimer and compared the data with the data ($J = -0.4$ cm^{-1}) for the analogous squarate-bridged ($C_4O_4^{2-}$) Ni(II) dimer. The approximately 40-fold decrease in J from the oxalate to the squarate was explained by the fact that the molecular orbitals of $C_4O_4^{2-}$ are stabilized more than those of $C_2O_4^{2-}$ and, consequently, the squarate ion orbitals interact less with the Ni(II) orbitals. Hoffmann et al.[7] concurred. Because we now have an oxalate-bridged Cu(II) dimer with a relatively large exchange interaction, we prepared the squarate analogue, $[Cu_2(Et_5dien)_2(C_4O_4)](BPh_4)_2$. This is the first reported example of a Cu(II) dimer bridged by the squarate ion. Susceptibility data for this compound are given in Table XVII[13] and Figure 11. It can be seen that there is a weak antiferromagnetic interaction with a μ_{eff} value of 1.41 μ_B at 4.2 K; least-squares fitting to eq 1 gives a J value of -2.1 cm^{-1} with $\bar{g}$ fixed at 2.145. This is a reduction of $\sim 1/18$ from the J value (-37 cm^{-1}) for the corresponding oxalate compound. Relative to the Ni(II) case, the smaller reduction in J value in replacing oxalate by squarate for the Cu(II) complexes probably partly reflects a reduced covalency in Cu–O interactions relative to Ni–O interactions. Also, because of differences in C–C bond distances (oxalate vs. squarate), the squarate ion has a smaller bite and this, coupled with the facility of the Cu(II) ion for distortions in coordination geometries, could lead to less reduction in J value. Thus, the Cu(II) ion "adjusts" its coordination geometry to enhance its interaction with the squarate ion. A comparison of the Q-band spectra of the oxalate (tracing B) and squarate (tracing C) compounds, as given in Figure 4, does point to a difference in ground-state geometries. There is a $\Delta M_S = 2$ transition ($\sim$0.001 times the $\Delta M_S = 1$ transition intensity) in the X-band spectrum of the squarate compound. Previously we reported[6] that the exchange interaction in a Ni(II) oxalate-bridged dimer is invariant to changes of counterions and *tetraamine* backside ligands. A sample of $[Ni_2(dien)_2(OH_2)_2(C_2O_4)](ClO_4)_2$, first reported by Curtis,[43] was prepared in this work and magnetic susceptibility data were collected (see Table XVIII[13]) to give, in a least-squares fitting,[44] a J value of -12 cm^{-1}. Thus, even though the Ni(II) ion coordination sphere now consists of a *triamine* and three oxygen atoms, the exchange interaction is essentially the same as found for the μ-oxalato-(nickel(II)–tetraamine) dimers.

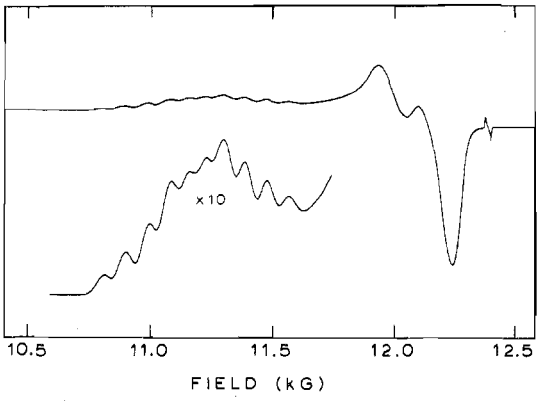

Figure 12. Q-Band (~35 GHz) EPR spectrum of a powdered sample of $[Cu_2(Me_5dien)_2(NCO)_2](BPh_4)_2$ recorded at ~300 K with DPPH as a frequency calibrant.

The succinate ion ($^-O_2CCH_2CH_2CO_2^-$) is related to the oxalate ion by the addition of an ethylene moiety. The C–C bond distance in the oxalate ion approaches that of a single bond. It is of interest to determine if the exchange interaction propagated by an oxalate ion depends only on the two carboxyl groups or if the C–C bond is active in the exchange interaction. Two compounds, $[Cu_2(Et_5dien)_2(O_2CCH_2CH_2CO_2)](BPh_4)_2$ and $[Cu_2(Me_5dien)_2(O_2CCH_2CH_2CO_2)](BPh_4)_2$, were prepared to modify the oxalate bridge to block exchange via the C–C bond. Inspection of Tables XIX[13] and XX[13] shows that, unfortunately, there are no signs of an exchange interaction with average μ_{eff} values of 1.85 (2) and 1.84 (1) μ_B, respectively. Table XI summarizes the EPR characteristics of these two compounds. There is no copper hyperfine structure to indicate an exchange interaction. There are $\Delta M_S = 2$ transitions in the X band at an intensity of 0.005 times the "full-field" transitions. Both compounds are quite soluble in solvents such as acetone and acetonitrile, indicating that the compounds are not polymeric. Two modes of dimer bridging can be suggested (L = Et_5dien or Me_5dien):

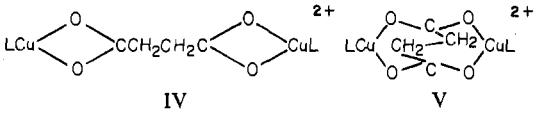

IV V

Structure IV would reduce the steric interactions with the methyl groups of L; this type of bridging is reported[45] for polymeric $Cu(O_2CCH_2CH_2CO_2)_2 \cdot 2H_2O$. Obviously, for our purposes we sought a Cu(II) dimer with structure V, and only when the structure of one of the compounds is in hand, will the absence of an exchange interaction in these compounds provide some insight into the oxalate-exchange problem.

Replacing the oxalate bridge by two cyanate ions (NCO^-) is another approach to investigating the involvement of the oxalate C–C bond in the exchange interaction. A sample of $[Cu_2(Me_5dien)_2(NCO)_2](BPh_4)_2$ was prepared. As summarized in Table XXI,[13] the compound shows a Curie law susceptibility with a μ_{eff} per Cu(II) ion of 1.84 (1) μ_B. The Q-band EPR spectrum in Figure 12 shows ten copper hyperfine lines on the parallel signal with spacings in the range from 69 to 94 G with an average of 83 G. This hyperfine structure clearly indicates the presence of an exchange interaction where ~ 0.02 cm$^{-1} < |J| < \sim 0.5$ cm^{-1}. The lower limit reflects the zero-field split, seven-line hyperfine structure, which results from an exchange interaction that is greater than

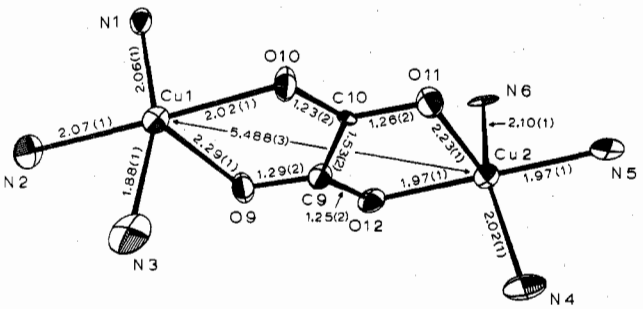

Figure 13. ORTEP plotting of the inner coordination sphere and oxalate bridge of $[Cu_2(dien)_2(C_2O_4)]^{2+}$ (perchlorate salt) using the crystallographic data of Waters et al.[11] The noncentrosymmetric structure has perchlorate ions semicoordinating to the Cu(II) ions in positions trans to O(9) and O(11).

the copper hyperfine interaction. The upper limit reflects the fact that no interaction is seen in the susceptibility down to 4.2 K. Analogous to the case of the oxalate compound, there are seven copper hyperfine lines visible on the $\Delta M_S = 2$ transition in the X-band spectrum. The two cyanate ions are most likely bridging in an end-to-end fashion as deduced from the similarity of the EPR spectrum to that for the analogous oxalate compound and the steric requirements of the Me_5dien ligand. This is one of the few oxygen-bonded transition metal cyanate complexes.[46] Of even greater importance to this work is the fact that, if the two cyanate ions can be considered as a pseudo-oxalate bridge missing the C–C bond, then it can be concluded that each carboxyl moiety of the oxalate bridge in $[Cu_2(Me_5dien)_2(C_2O_4)](BPh_4)_2$ can, in and of itself, propagate an exchange interaction.

Magnetic Exchange Mechanism. Several factors probably determine the range of exchange interactions observed for $[Cu_2(\text{"dien"})_2(C_2O_4)]X_2$ when the triamine ligand and counterion are changed. It is instructive to take a look at a simplified molecular orbital description of the exchange interaction in such an oxalate-bridged Cu(II) dimer. More particularly, an attempt will be made to explain, in molecular orbital terms, the differences in magnetic exchange mechanism for Cu(II) dimers having either structure I or structure II. As mentioned above, these two structures are exemplified by the dimeric cations in $[Cu_2(Et_5dien)_2(C_2O_4)](BPh_4)_2$ and $[Cu_2(dien)_2(C_2O_4)](ClO_4)_2$, respectively. The bond distances and angles in $[Cu_2(Et_5dien)_2(C_2O_4)]^{2+}$ can be reviewed in Figure 1 and Table V. In Figure 13 the inner coordination sphere in the noncentrosymmetric dimer in $[Cu_2(dien)_2(C_2O_4)](ClO_4)_2$ is shown with the appropriate bond distances. The internal oxalate distances are relatively constant in the two structures. In the TBP Et_5dien complex, the oxalate bite (i.e., the O–Cu–O angle) is 80.2° while in the SP dien complex the average bite is 79°. The O–C–O angles are 125.7° in the Et_5dien compound and 121 and 127° in the dien complex. All other angles differ by ~3° or less and, taken together, these data support the fact that the dimensions of the oxalate dianion are relatively constant in the two salts. The difference in exchange interactions in $[Cu_2(Et_5dien)_2(C_2O_4)](BPh_4)_2$ ($J = -37$ cm^{-1}) and $[Cu_2(dien)_2(C_2O_4)](ClO_4)_2$ ($|J| < 0.5$ cm^{-1}) is due, then, to the difference in Cu(II) ion coordination geometry as influenced by the backside triamine ligand.

Hoffmann et al.[7] have shown that, with a molecular orbital analysis, the antiferromagnetic contribution to a magnetic exchange interaction can be analyzed in terms of pairwise interactions of dimeric orbitals. In a Cu(II) dimer, each Cu(II) ion has one unpaired electron in an essentially d-type orbital and, to first order, the antiferromagnetic interaction reflects the level of interaction of the two unpaired-electron orbitals, one at each Cu(II) ion. The interaction between the two Cu(II) d orbitals is effected by an interaction with the

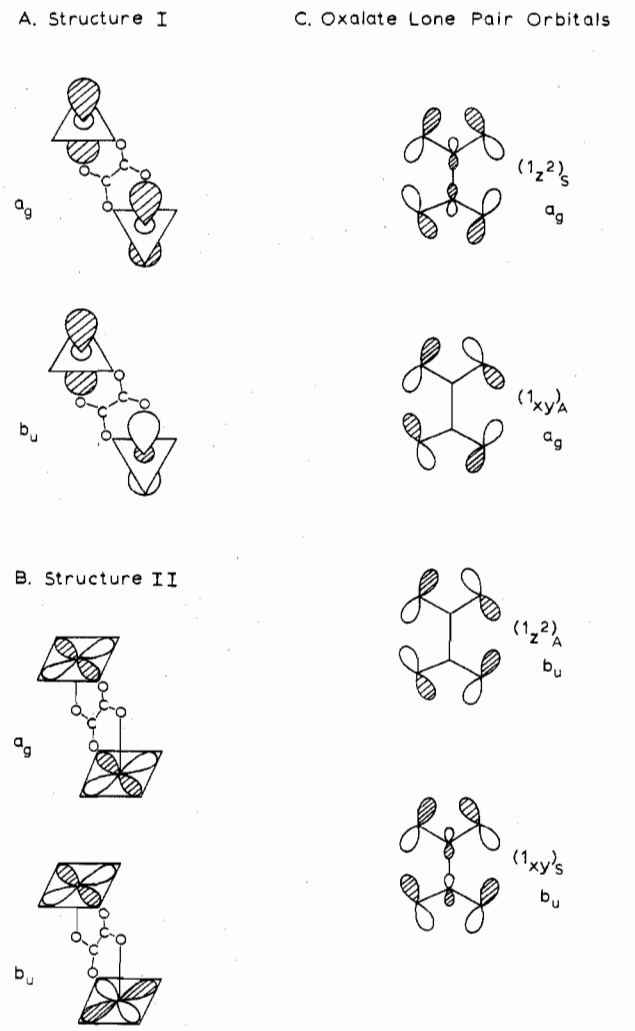

Figure 14. Symmetry-adapted combinations of unpaired-electron Cu(II) ion orbitals and oxalate lone-pair molecular orbitals.

appropriate molecular orbitals of the bridging group. The TBP Cu(II) ions in a dimer with structure I have d_{z^2} ground states, whereas the SP Cu(II) ions in a dimer with structure II have $d_{x^2-y^2}$ ground states. In the former case, then, we are concerned with the energy difference between the two dimer molecular orbitals which form as symmetric (a_g in C_{2h} symmetry) and antisymmetric (b_u in C_{2h} symmetry) combinations of the two (essentially) d_{z^2} orbitals. These two combinations are sketched in the upper left part of Figure 14. The symmetric (a_g) and antisymmetric (b_u) combinations of two $d_{x^2-y^2}$ orbitals are also pictured for structure II. These symmetry combinations of d orbitals interact with the appropriate oxalate orbitals. Following Hoffmann's lead, we only consider the four lone-pair orbitals of $C_2O_4^{2-}$ and these are also sketched in Figure 14, where the four orbitals are ordered in energy with the lowest being the most stable. The oxalate orbitals are labeled as before.[7] It is these four lone-pair orbitals that provide the greatest interaction with the prescribed combinations of d orbitals and lead to an energy difference between a pair of symmetric and antisymmetric orbitals.

In the case of structure I, the a_g (symmetric) combination of d_{z^2} orbitals could by symmetry interact with either of the oxalate a_g orbitals; however, the overlap with the $(1_{xy})_A$ orbital is the best. That is, each "bite" of this oxalate orbital has both orbital phases present, which allows at each Cu(II) ion a simultaneous interaction with one axial lobe and the equatorial ("doughnut") lobe of the Cu(II) d_{z^2} atomic orbital. The $(1_{xy})_A$ orbital is antibonding relative to the through-space O–O interaction. On the other hand, the b_u combination of d_{z^2}

orbitals will interact with both of the b_u oxalate orbitals. It is to be noted that the $(1_{xy})_S$ orbital has the greater O–O interaction in each carboxyl moiety and that there is a node in the C–C interaction. As a result of the interactions of the oxalate orbitals with the a_g and b_u combinations of d_{z^2} orbitals an energy difference will develop between the a_g and b_u combinations. In the above analysis the antiferromagnetic interaction ($J = -37$ cm^{-1}) in $[Cu_2(Et_5dien)_2(C_2O_4)](BPh_4)_2$ results from the d_{z^2} orbitals interacting via the two carboxyl moieties of $C_2O_4^{2-}$. The interaction is propagated by through-space O–O interaction and the C–C single bond is not appreciably involved.

Inspection of the two combinations of $d_{x^2-y^2}$ orbitals for structure II points to a possible cause for the weak ($|J| < \sim 0.5$ cm^{-1}) exchange interaction found for $[Cu_2(dien)_2(C_2O_4)](ClO_4)_2$. If the exchange is propagated by the carboxyl moieties, the interaction develops from an equatorial site of one Cu(II) ion through one carboxyl unit to the axial site of the other Cu(II) ion. None of the four oxalate orbitals pictured in Figure 14 overlaps to any degree with a $d_{x^2-y^2}$ orbital in the axial direction. Only one of the orbitals has some C–C bonding character; however, there are nodes in this molecular orbital between the carbon and oxygen atomic orbitals. Thus, there also does not seem to be opportunity for an exchange pathway from an equatorial site of one Cu(II) ion through the C–C bond to an equatorial site of the other Cu(II) ion. The oxalate bridge does not present the proper lone-pair orbitals to effect an appreciable antiferromagnetic exchange interaction in dimer II.

From the above discussion it is possible to understand why changing the backside ligand of an oxalate-bridged Cu(II) dimer can dramatically affect the magnitude of the exchange interaction. All of the Et_5dien complexes have TBP Cu(II) coordination geometries with d_{z^2} ground states and for a given counterion the Et_5dien dimers exhibit the greatest antiferromagnetic interactions. With the other triamines (i.e., Me_5dien, dien, and dpt) as backside ligands a variety of distorted SP geometries predominate and the compounds have EPR spectra that are consistent with a $d_{x^2-y^2}$ ground state. These compounds have weaker antiferromagnetic interactions.

There are several other factors that could influence the exchange interaction in these compounds. There is probably a variability in ligand field strengths for the series of triamines used. For example, it would be expected that in the alkylation of dien to give Me_5dien the basicity of the triamine would increase and this could increase the ligand field strength of the ligand. An increased ligand field splitting would displace the d_{z^2} and $d_{x^2-y^2}$ orbitals to higher energy. Their interaction with the oxalate orbitals would be decreased with a concomitant decrease in antiferromagnetic exchange interaction.

Perusal of Table XI shows that there is an anion dependence of the magnitude of antiferromagnetic exchange. In all instances, the greatest interaction is found for the oxalate-bridged Cu(II) dimers with noncoordinating BPh_4^- counterions. The attenuation in the interaction with the ClO_4^- and PF_6^- counterions apparently is derived from the ability of these ions to semicoordinate to the Cu(II) ions to give pseudooctahedral complexes. The $[Cu_2(dien)_2(C_2O_4)]^{2+}$ cation depicted in Figure 13 actually has oxygen atoms of the ClO_4^- counterions weakly bonding in the Cu(II) coordination positions trans to O(9) and O(11) at distances of 2.96 and 2.78 Å, respectively. The semicoordination of ClO_4^- could somewhat change the characteristics of the orbital at each Cu(II) ion in which the unpaired electron resides and decrease the overlap with the oxalate orbitals. The semicoordination of ClO_4^- will also increase the ligand field splitting, displacing the $d_{x^2-y^2}$ orbital to higher energies with a resultant decrease in interaction with the oxalate orbitals. The influence of semicoordination of ClO_4^- has very recently been noted[47] for the two crystalline forms of the di-μ-hydroxo-bridged $[Cu(DMAEP)OH]_2(ClO_4)_2$, where DMAEP is 2-(2-dimethylaminoethyl)pyridine. In the β form each ClO_4^- semicoordinates to *one* Cu(II) ion giving a five-coordinate SP coordination geometry. In this form J was found to be -100 cm^{-1}, which fits the $2J$ vs. ∠Cu–O–Cu correlation. In the α form each ClO_4^- acts as a bidentate ligand and bridges between the two Cu(II) ions. This results in a distorted octahedral coordination geometry. According to the $2J$ vs. ∠Cu–O–Cu correlation, this α compound should have a J value of -25 cm^{-1}; however, J was found to be only -2.4 cm^{-1}.

Yet another factor must be considered to explain the magnetic exchange interactions in the μ-oxalato-copper(II) dimers. A displacement of the Cu(II) ion from either the trigonal (TBP geometry) or basal (SP geometry) plane would affect an exchange interaction. In $[Cu_2(Et_5dien)_2(C_2O_4)]^{2+}$ each TBP Cu(II) ion is out of the O(2)–N(2)–N(3) plane (Figure 1) by only 0.0045 Å, while in $[Cu_2(dien)_2(C_2O_4)]^{2+}$ the displacements from the SP planes are 0.115 and 0.188 Å for Cu(1) and Cu(2), respectively. This difference in displacements from coordination planes would lead to a difference in overlaps with the oxalate orbitals and, consequently, a difference in antiferromagnetic coupling. Hence, if $[Cu_2(Et_5dien)_2(C_2O_4)](BPh_4)_2$ and $[Cu_2(dien)_2(C_2O_4)](BPh_4)_2$ have dimeric cations that approximate structures I and III, respectively, then the decrease in the antiferromagnetic coupling from -37.4 and -7.3 cm^{-1}, respectively, for these complexes to -5.7 and -3.4 cm^{-1} for the dpt and Me_5dien analogues can be attributed to a movement of the Cu(II) ions further out of the basal plane in these later two complexes. This would be consistent with the coordinating tendencies of the dpt and Me_5dien ligands as compared to those of the dien ligand. That is, relative to dien, increasing the size of the chelate ring (ethylene to propylene linkages) or substituting bulky methyl groups for nitrogen hydrogen atoms distorts the amine nitrogen coordination from a square plane.

Conclusions

Dimeric Cu(II) complexes of the form $[Cu_2(\text{"dien"})_2(C_2O_4)]X_2$ have been characterized by EPR and variable-temperature magnetic susceptibility. Structural data for the oxalate-bridged dimers in $[Cu_2(Et_5dien)_2(C_2O_4)](BPh_4)_2$ and $[Cu_2(dien)_2(C_2O_4)](ClO_4)_2$ show that the dimensions of the oxalate bridges are the same and that the change in exchange interaction from -37 cm^{-1} to less than 0.5 cm^{-1}, respectively, is due to several factors. The local Cu(II) ion coordination geometry, as enforced by the "dien" ligand, is shown with a molecular orbital analysis to be important in determining the level of antiferromagnetic exchange, which apparently is propagated by through-space O–O interactions in the carboxyl moieties of the oxalate bridge. Very little involvement of the oxalate C–C single bond in the superexchange is indicated. The displacement of the Cu(II) ion from a given coordination plane is important. And, finally, changing the counterion X^- leads to a change in exchange interaction, possibly due to semicoordination of certain anions.

Acknowledgment. We thank R. G. Wollmann for use of his computer program for least-squares fitting of magnetic susceptibility data. We are grateful for support from National Institutes of Health Grant HL 13652 and for computing funds from the University of Illinois Research Board.

Registry No. $[Cu_2(Et_5dien)_2(C_2O_4)](BPh_4)_2$, 61651-88-5; $[Cu_2(Me_5dien)_2(C_2O_4)](BPh_4)_2$, 61951-14-2; $[Cu_2(dpt)_2(C_2O_4)](BPh_4)_2$, 61951-15-3; $[Cu_2(Et_5dien)_2(C_2O_4)](ClO_4)_2$, 61990-14-5; $[Cu_2(Me_5dien)_2(C_2O_4)](ClO_4)_2$, 62057-29-8; $[Cu_2(dpt)_2(C_2O_4)](ClO_4)_2$, 21268-18-8; $[Cu_2(Et_5dien)_2(C_2O_4)](PF_6)_2$, 61990-15-6; $[Cu_2(Me_5dien)_2(C_2O_4)](PF_6)_2$, 62057-30-1; $[Cu_2(dpt)_2(C_2O_4)](PF_6)_2$, 61951-16-4; $[Cu_2(dien)_2(C_2O_4)](PF_6)_2$, 61990-16-7; $[Cu_2$-

$(Et_5dien)_2(C_4O_4)](BPh_4)_2$, 62067-41-8; $[Cu_2(Et_5dien)_2(O_2CCH_2CH_2CO_2)](BPh_4)_2$, 62067-39-4; $[Cu_2(Me_5dien)_2(O_2CCH_2CH_2CO_2)](BPh_4)_2$, 62067-37-2; $[Cu_2(Me_5dien)_2(NCO)_2](BPh_4)_2$, 62015-68-3; $[Cu_2(Et_5dien)_2(NCO)_2](BPh_4)_2$, 61966-58-3; $[Cu_2(dpt)_2(NCO)_2](BPh_4)_2$, 61966-60-7; $[Ni_2(dien)_2(OH_2)_2(C_2O_4)](ClO_4)_2$, 62015-63-8.

Supplementary Material Available: Tables I (analytical data), IV (anisotropic thermal parameters for $[Cu_2(Et_5dien)_2(C_2O_4)](BPh_4)_2$), VI (least-squares planes for the same compound), VII–X (experimental and calculated magnetic susceptibility data for BPh_4^- salts of Et_5dien, Me_5dien, and dpt compounds), and XII–XXI (experimental and calculated magnetic susceptibility data for three ClO_4^- and four PF_6^- salts of μ-oxalato-copper(II) compounds, one squarate-bridged Cu(II) compound, two succinate-bridged Cu(II) compounds, one oxalate-bridged Ni(II) compound, and one cyanate-bridged Cu(II) compound) and final values of $|F_o|$ and $|F_c|$ for $[Cu_2(Et_5dien)_2(C_2O_4)](BPh_4)_2$ (28 pages). Ordering information is given on any current masthead page.

References and Notes

(1) Camille and Henry Dreyfus Fellow, 1972–1977; Alfred P. Sloan Fellow, 1976–1978.
(2) (a) W. E. Hatfield, *ACS Symp. Ser.*, **No. 5**, 108–141 (1974); (b) W. E. Hatfield in "Theory and Applications of Molecular Paramagnetism", E. A. Boudreaux and L. N. Mulay, Ed., Wiley-Interscience, New York, N.Y., 1976, pp 349–449; (c) V. H. Crawford, H. W. Richardson, J. R. Wasson, D. J. Hodgson, and W. E. Hatfield, *Inorg. Chem.*, **15**, 2107 (1976); (d) a correlation between 2J and the Cu–Cl–Cu bridging angle has been suggested very recently: W. E. Estes, J. R. Wasson, J. W. Hall, D. J. Hodgson, and N. E. Hatfield, Abstracts, 173rd National Meeting of the American Chemical Society, New Orleans, La., March 1977, No. INOR 61.
(3) D. J. Hodgson, *Prog. Inorg. Chem.*, **19**, 173 (1975).
(4) (a) M. D. Glick and R. L. Lintvedt, *Prog. Inorg. Chem.*, **21**, 233 (1976); (b) R. L. Lintvedt, M. D. Glick, B. K. Tomlonovic, D. P. Gavel, and J. M. Kuszaj, *Inorg. Chem.*, **15**, 1633 (1976).
(5) E. J. Laskowski, T. R. Felthouse, D. N. Hendrickson, and G. J. Long, *Inorg. Chem.*, **15**, 2908 (1976).
(6) D. M. Duggan, E. K. Barefield, and D. N. Hendrickson, *Inorg. Chem.*, **12**, 985 (1973).
(7) P. J. Hay, J. C. Thibeault, and R. Hoffmann, *J. Am. Chem. Soc.*, **97**, 4884 (1975).
(8) G. R. Hall, D. M. Duggan, and D. N. Hendrickson, *Inorg. Chem.*, **14**, 1956 (1975).
(9) D. M. Duggan and D. N. Hendrickson, *Inorg. Chem.*, **12**, 2422 (1973).
(10) R. F. Ziolo, M. Allen, D. D. Titus, H. B. Gray, and Z. Dori, *Inorg. Chem.*, **11**, 3044 (1972).
(11) N. F. Curtis I. R. N. McCormick, and T. N. Waters, *J. Chem. Soc., Dalton Trans.*, 1537 (1973).
(12) T. R. Felthouse, E. J. Laskowski, D. S. Bieksza, and D. N. Hendrickson, *J. Chem. Soc., Chem. Commun.*, 777 (1976).
(13) Supplementary material.
(14) N. F. Curtis, *J. Chem. Soc. A*, 1584 (1968).
(15) R. West and H. Y. Niu, *J. Am. Chem. Soc.*, **85**, 2589 (1963).
(16) B. N. Figgis and J. Lewis, *Mod. Coord. Chem.*, 403 (1960).
(17) P. W. Selwood, "Magnetochemistry", 2nd ed, Interscience, New York, N.Y., 1956, pp 78, 92–93.
(18) B. Bleaney and K. D. Bowers, *Proc. R. Soc. London, Ser. A*, **214**, 451 (1952).
(19) J. P. Chandler, Program 66, Quantum Chemistry Program Exchange, Indiana University, Bloomington, Ind., 1973.
(20) (a) H. P. Hansen, F. Herman, J. D. Lea, and S. Skillman, *Acta Crystallogr.*, **17**, 1040 (1964); (b) D. T. Cromer, and J. B. Mann, *Acta Crystallogr., Sect. A*, **24**, 321 (1968); (c) "International Tables for X-Ray Crystallography", Vol. III, Kynoch Press, Birmingham, England, 1962.
(21) D. M. Duggan and D. N. Hendrickson, *Inorg. Chem.*, **13**, 1911 (1974).
(22) (a) F. S. Stephens *J. Chem. Soc. A*, 883 (1969); (b) *ibid.*, 2233 (1969); (c) *ibid.*, 2493 (1969); (d) G. Davey and F. S. Stephens, *ibid.*, 103 (1971).
(23) (a) M. Cannas, G. Carta, and G. Marongiu, *J. Chem. Soc., Dalton Trans.*, 553 (1974); (b) *ibid.*, 556 (1974).
(24) S. C. Yang and P. W. R. Corfield, Abstracts, American Crystallographic Association Meeting, University of Connecticut, 1973, No. M8.
(25) (a) T. J. Kistenmacher, T. Sorrell, and L. G. Marzilli, *Inorg. Chem.*, **14**, 2479 (1975); (b) T. Sorrell, L. G. Marzilli, and T. J. Kistenmacher, *J. Am. Chem. Soc.*, **98**, 2181 (1976).
(26) Z. Dori, R. Eisenberg, and H. B. Gray, *Inorg. Chem.*, **6**, 483 (1967).
(27) C. G. Pierpont, D. N. Hendrickson, and L. C. Francesconi, submitted for publication in *Inorg. Chem.*
(28) M. DiVaira and P. L. Orioli, *Chem. Commun.*, 590 (1965).
(29) (a) G. A. Barclay, B. F. Hoskins, and C. H. L. Kennard, *J. Chem. Soc.*, 5691 (1963); (b) P. C. Jain and E. C. Lingafelter, *J. Am. Chem. Soc.*, **89**, 724 (1967); (c) N. A. Bailey, E. D. McKenzie, and J. R. Mullins, *Chem. Commun.*, 1103 (1970); (d) E. J. Laskowski, D. M. Duggan, and D. N. Hendrickson, *Inorg. Chem.*, **14**, 2449 (1975).
(30) (a) M. A. Viswamitra, *Z. Kristallogr., Krlstallgeom., Kristallchem., Kristallphys.*, **117**, 437 (1962); (b) T. Weichert and J. Löhn, *ibid.*, **139**, 223 (1974); (c) W. Pannhorst and J. Löhn, *ibid*, **139**, 236 (1974); (d) M. A. Viswamitra, *J. Chem. Phys.*, **37**, 1408 (1962); (e) J. Garaj, *Chem. Commun.*, 904 (1968); (f) J. Löhn, *Acta Crystallogr., Sect. A*, **25**, S121 (1969); (g) J. Garaj, H. Langfelderova, G. Lundgren, and J. Gazo, *Collect. Czech. Chem. Commun.*, **37**, 3181 (1972); (h) L. Cavalca, A. C. Villa, A. G. Manfredotti, A. Mangia, and A. A. G. Tomlinson, *J. Chem. Soc., Dalton Trans.*, 391 (1972); (i) J. Korvenranta *Suom. Kemistil. B*, **46**, 296 (1973).
(31) D. J. Hodgson and J. A. Ibers, *Acta Crystallogr., Sect. B*, **25**, 469 (1969).
(32) A. Robbins, G. A. Jeffrey, J. P. Chesick, J. Donohue, F. A. Cotton, B. A. Frenz, and C. A. Murillo, *Acta Crystallogr., Sect. B*, **31**, 2395 (1975).
(33) C. Glidewell and G. M. Sheldrick, *J. Chem. Soc. A*, 3127 (1971).
(34) P. C. Chieh, *J. Chem. Soc. A*, 3243 (1971).
(35) F. A. Cotton and C. A. Murillo, *Inorg. Chem.*, **14**, 2467 (1975).
(36) For guidelines on possible geometries which can be inferred from various g values, see B. J. Hathaway and D. E. Billing, *Coord. Chem. Rev.*, **5**, 143 (1970).
(37) T. D. Smith and J. R. Pilbrow, *Coord. Chem. Rev.*, **13**, 173 (1974).
(38) C. P. Slichter, *Phys. Rev.*, **99**, 479 (1955).
(39) Proposed and crystallographically characterized Cu^{II}–dien complexes are described in ref 8.
(40) M. Cannas, G. Carta, A. Cristini, and G. Marongiu, *J. Chem. Soc., Dalton Trans.*, 1278 (1974).
(41) M. Cannas, G. Carta, and G. Marongiu, *Gazz. Chim. Ital.*, **104**, 581 (1974).
(42) B. W. Skelton, T. N. Waters, and N. F. Curtis, *J. Chem. Soc., Dalton Trans.*, 2133 (1972).
(43) N. F. Curtis, *J. Chem. Soc.*, 4109 (1963).
(44) The equations used to fit susceptibility data for Ni(II) systems are given in ref 6. In addition to $J = -12.2$ cm^{-1}, the other fitting parameters are $g = 2.07$, $D = 14.8$ cm^{-1}, and $Z'J' = 0.29°$. The fitting criterion SE was found to be 0.050 and the TIP was taken as 200×10^{-6} cgsu/dimer.
(45) B. H. O'Connor and E. N. Maslen, *Acta Crystallogr.*, **20**, 824, 1966).
(46) (a) D. M. Duggan and D. N. Hendrickson, *Inorg. Chem.*, **13**, 2056 (1974); (b) D. M. Duggan and D. N. Hendrickson, *ibid.*, **13**, 2929 (1974).
(47) K. T. McGregor, D. J. Hodgson, and W. E. Hatfield, *Inorg. Chem.*, **15**, 421 (1976).